4-2019

Enhanced MPPT Controllers for Smart Grid Applications

Mohamed Khallaf
mxk9246@rit.edu

RIT

Enhanced MPPT Controllers for Smart Grid Applications

by

Mohamed Khallaf

A Thesis Submitted in Partial Fulfillment of the

Requirements for the Degree of Master of Science in Electrical Engineering

Department of Electrical Engineering and Computing Sciences

Rochester Institute of Technology, Dubai UAE

April 2019

Enhanced MPPT Controllers for Smart Grid Applications

by

Mohamed Khallaf,

A Thesis Submitted in Partial Fulfillment of the Requirements

for the Degree of Master of Science in Electrical Engineering

Department of Electrical Engineering and Computing Sciences

Approved By:

_____Date:_____

Dr. Abdulla Ismail

Thesis Advisor – Department of Electrical Engineering

_____Date:_____

Dr. Yousef Al Assaf

Committee Member – Department of Electrical Engineering

_____Date:_____

Dr. Mohamed Samaha

Committee Member – Department of Mechanical Engineering

Acknowledgements

I would like to express the deepest appreciation to Dr. Abdulla Ismail, my thesis advisor, for his tremendous guidance and encouragement. Dr. Abdulla has been instrumental for the success of my thesis and I am honored to have had him as my advisor.

Besides my advisor, I would like to thank the rest of my thesis committee: Dr. Yousef Al Assaf, President of RIT Dubai and Dr. Mohamed Samaha, Professor of Mechanical Engineering at RIT Dubai, on their insightful comments which allowed me to widen my research from various perspectives.

Last but not least, I would like to express my gratitude to my family: my parents and sisters for their endless support and motivation throughout this journey. Without them this thesis would not have been possible.

Dedicated to my family.

Table of Contents

List of Figures

List of Tables

List of Abbreviations

AC	Alternate Current
DC	Direct Current
FLC	Fuzzy Logic Control
FIS	Fuzzy Inference System
INC	Incremental Conductance
IR	Integral Regulator
I-V	Current-Voltage
MF	Membership Function
MPP	Maximum Power Point
MPPT	Maximum Power Point Tracking
PV	Photovoltaic
PWM	Pulse Width Modulation
P&O	Perturb and Observe
P-V	Power-Voltage

List of Publications

- M. Khallaf and A. Ismail, "Design and Simulation of Enhanced MPPT Algorithms for Photovoltaic Systems", 10th IEEE GCC CONFERENCE, Kuwait, April 2019.
- M. Khallaf and A. Ismail, "Design of Photovoltaic System using Fuzzy Logic Controller", International Research Journal of Engineering and Technology (IRJET), Volume 6 Issue 4, April 2019, S.NO: 296

Abstract

Over the past years, the energy demand has been steadily growing and so methods of how to cope with this staggering increase are being researched and utilized. One method of injecting more energy to the grid is renewable energy, which has become in recent years an integral part of any country's power generation plan. Thus, it is a necessity to enhance renewable energy resources and maximize their grid utilization, so that these resources can step up and reduce the over dependency of global energy production on depleting energy resources.

This thesis focuses on solar power and effective means to enhance its efficiency through the use of different controllers. In this regard, substantial research efforts have been done. However, due to the current market and technological development, more options are made available that are able to boast the efficiency and utilization of renewables in the power mix.

In this thesis, an enhanced maximum power point tracking (MPPT) controller has been designed as part of a Photovoltaic (PV) system to generate maximum power to satisfy load demand. The PV system is designed and simulated using MATLAB (consisting of a solar panel array, MPPT controller, boost converter, and a resistive load). The solar panel chosen for the array is Sun Power SPR- 440NE-WHT-D and the array is designed to produce 150 kW of power. The MPPT controller is designed using three different algorithms and the results are compared to identify each controller's fortes and drawbacks. The three designed controllers used are based on Perturb and Observe (P&O) algorithm, Incremental Conductance (INC) with an Integral Regulator (IR) and Fuzzy Logic Control (FLC). Each controller was tested under two different scenarios; the first is when the panel array is subjected to constant

amount of solar irradiance along with a constant atmospheric temperature and the second scenario has varying solar irradiance and atmospheric temperature. The performance of these controllers is analyzed and compared in terms of the output power efficiency, system dynamic response and finally the oscillations behavior. After analyzing the results, it is shown that Fuzzy Logic Controller design performed better compared to the other controllers as it had in most cases the highest mean power efficiency and fastest response.

Chapter 1 Introduction

1.1 Motivation

With the exponential growth in the human population and the expansion of cities throughout the world, a predicament was born. How can electricity be supplied to these new areas when the traditional grid is already failing at the current level of load? The traditional energy system is becoming more and more unreliable by the day with the increase in power outages, coal prices, greenhouse gas emissions and the amount of electricity wasted during transmission through the grid for reasons ranging from poor human oversight to natural disasters. Power blackouts are becoming a massive burden and complication on the traditional grid. A power blackout is a failure to deliver electricity to a certain area for a period of time and according to the US Government, power outages and power quality issues cost American businesses more than $100 billion on average each year [1]. It is also reported that the one-hour outage in Chicago in 2000 resulted in $20 trillion in trades being delayed.

This has lead researchers to focus on developing new energy technologies that are more reliable, robust, and have the ability to reduce the gas emissions and the loss of electric power. Hence, the idea of Smart Grid was developed. This chapter describes Smart Grids, examines their components, structure, and discusses their benefits and challenges. This thesis focuses on the power generation components in smart grids using solar energy.

1.2 Research Objectives

The objectives of this research are summarized as follows:

1. Designing an enhanced PV system that produces an output of 150 kW and simulating it using a PV panel that is widely used in the industry (Sun Power SPR- 440)
2. Designing three MPPT controllers: Perturb & Observe, Incremental Conductance with Integral Regulator, and Fuzzy Logic.
3. Modeling and simulating the designed PV system using the three MPPT controllers and compare their responses under constant and varying weather conditions.
4. Studying the effect of increasing temperature and reducing irradiance on the system output power.

1.3 Thesis Organization

This Thesis is divided into six chapters, as follows:

- Chapter 1 describes the motivation behind this thesis and its objectives.
- Chapter 2 discusses the literature review behind Smart Grids and its main components, especially the PV system, which is the main focus of this thesis.
- Chapter 3 discusses the three MPPT controllers used in this thesis, which are P&O, INC+IR, and FLC.
- Chapter 4 shows the design of the PV system (PV Panel, MPPT, and DC-DC Converters).
- Chapter 5 illustrates the results produced from each MPPT controller under both constant and varying weather conditions.
- Chapter 6 summarizes the work done and the results obtained along with some recommendations for further work.

Chapter 2 Problem Background

2.1 Introduction

This chapter introduces two main topics, smart grids and renewable energy resources (especially photovoltaic systems). It also highlights the structure, usage, and challenges of implementing each of them individually.

2.2 Introduction to Smart Grids

According to the U.S. Department of Energy, a Smart Grid is a digital technology that allows two-way communication between consumers and the utility company. It also makes use of the new control, automation, sensing, and communication technologies integrated together to react to the unpredictable demand for electricity digitally and without the aid of humans [2]. The National Electrical Manufacturers Association (NEMA) also added a crucial point to the definition of Smart Grids, unlike the traditional system, Smart Grids can take advantage of new technologies such as distributed generation, renewable energy (solar, wind, etc.), smart metering, demand side management systems, and distribution automation [3].

Smart Grids can also be used to combat all of the problems that emanate from the use of a traditional grid due to the following features [1]:

- Smart Grid is intelligent due to its ability to anticipate and deal with overloads autonomously and quicker than the workers would respond, which can lead to decreasing or even averting power blackouts.
- Smart Grid is efficient as it can sense wastage in electricity and also keep up with the ever-increasing demand in electricity without introducing extra power lines.

- Smart Grid can accommodate renewable energy because it can smoothly integrate any type of energy resource such as renewable energy sources to handle part of the load and thus limiting the usage of coal and natural gas, which will reduce our carbon footprint.
- Smart Grid is engaging as it actively links the consumer with the utility company, which allows the consumer to control their power consumption in terms of price and source of power (coal, solar, etc.)
- Smart Grid is resilient as it is more distributed than centralized and with the inclusion of the safety procedures it becomes a lot more withstanding.
- Finally, Smart Grid is more environmentally friendly due to the advanced technologies incorporated within renewable energy sources that can now be easily integrated with the grid thus reducing the CO2 emissions and global warming.

The basic requirements of a Smart Grid are: (i) integrated communication platform that can interconnect all the different components in the system and allow for the exchange of data; (ii) an abundance of sensors and measuring devices to record every action precisely and in real time for the use of either the utility company or the consumer; (iii) advanced control and automation techniques to correctly predict the ever-changing demand for electricity and to be able to cope and react to any unforeseen event swiftly; (iv) latest technology in energy storage and electronics to amplify the overall performance and efficiency of the system; and (v) a high-level software or artificial intelligence (AI) based system to gather information, decide which course of action is needed to be taken and relay it to the system.

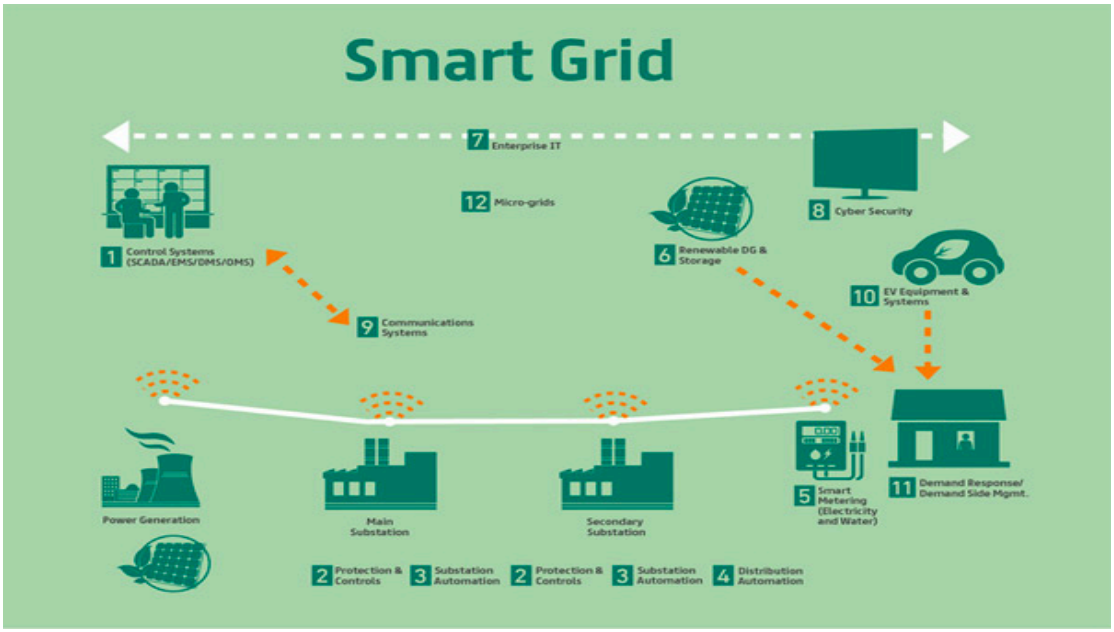

Figure 2.1 Smart Grid Components [4]

The components of a Smart Grid, shown in Figure 2.1, can be summarized as follows [5]:

(i) Sensors: these components need to be placed across the network on each transmission line and transformer. There are many types of sensors such as voltage, current, temperature, and fault indication to keep the workers alert on what is going on during transmission at all times. This information will be sent back to the monitoring station over the wireless communication system.

(ii) Communication System: this system would need to be a WAN (Wide Area Network) to be able to cover all the distance from the generation station to the end of the line whether it is a house, commercial building, government entity or an industrial site.

(iii) Distribution Management system: this component includes Distribution Automation, Distribution Generation, Fault Management and other supervisory purposes. This part of the grid is a very critical part as it is the

starting point from which the consumer gets electricity; therefore, there are a lot of variables that need monitoring and optimizing. This part of the grid will be sending out data regarding power generation, power quality, power flow, the usual measurements of voltage and current, and finally the status of the advanced electronics used in the system all in real time, which necessitates handling this system with additional caution and upkeep.

(iv) Control Technology is needed to adapt to a calculated switching operations of the network as well as a deliberate isolation or cutting off power during the times of low demand for electricity. At first, the task handled by the control system may seem simple, but this system needs to be of a high dependability and promptness. During sudden emergencies, ones that take precedence over regular and daily functions; the control technology used should be able to adjust itself to shoulder its daily functions along with the emergency response immediately to prevent a catastrophe from occurring.

(v) Advanced Metering Infrastructure (AMI): which are smart meters situated at the consumers' place. This advanced technology also uses the wireless communication function to provide the utility company with real-time data regarding power consumption and power irregularities so that it can predict and act accordingly ahead of time. It also benefits the user as it provides data about the change in price depending on time and also regarding future power outages.

Table 2.1 shows main differences between the conventional Grids and Smart Grids. The transformation from an electromechanical system into a digital system along with

the addition of a communication infrastructure that allows for a two-way communication between the utility company and the consumer, paved the way towards modernizing and revolutionizing the Grid.

Table 2.1 Comparison of Conventional and Smart Grids

Conventional	Smart
Electromechanical	Digital
One-way communication	Two-way communication
Centralized generation	Distributed generation
Few sensors	More sensors
Manual monitoring	Self-monitoring
Manual restoration	Automatic restoration
Failures and blackouts	Adaptive and resilient
Limited control	Full control
Few customer choices	Wider customer choices

The integration of sensors and monitors throughout the system has helped in optimizing the reaction time as well as increasing the efficiency of the whole system when it comes to power wastage and cutting costs. It has also helped elevate the quality of power supplied to the consumer as it can easily match the high standards and expectations that people have. Another critical advantage is that it can automatically detect, respond to, and even prevent disturbances in the transmission and distribution part of the system, so that it minimizes or eliminates the impact on the consumer. Moreover, Smart Grid is more robust than the conventional grid as it can withstand attacks and natural disasters due to its quick self-restoration feature as well as its distributed generation system that will keep the attack localized and will not affect the other areas.

Smart Grid will also help in integrating the technologies of the 21st Century such as electric and hybrid cars due to the integration of renewable energy as well as advanced storage technologies that will allow us access to plug-in from virtually everywhere [6]. Finally, a subtle benefit of implementing Smart Grids is that it actually opens up a new space in a market that is becoming more and more saturated by the day. Should Smart Grids be implemented heavily in the future, this will cause a huge demand worldwide: a demand for electronics, communication, control technologies, and also human capital. Smart Grids are considered an immense investment and commitment that will not only gear us towards a better future but will also change the lives of all people right now from the lowest ranking worker to the biggest investing company. Everyone will have a chance to improve his or her quality of life.

2.2.1 Challenges of a Smart Grid

Even though Smart Grids have the capability of transforming the electric energy market, designing and implementing it are two different things. There are some challenges that need to be tackled after committing to the decision of improving their grid structure. Some palpable challenges are the high initial cost and the amount of time needed to transform the grid. Another challenge is the advanced technology factor. Smart Grids depend hugely on advanced technologies in every field: electronics, communication, control and automation, AMI, storage devices, and software-wise as well. These kinds of technologies are hard to come by as they are either very costly, or hard to acquire or purchase.

Furthermore, another major challenge is cyber security. With the grid transformed into a digital one and everything being controlled or monitored wirelessly, the threat of having someone hack into it is now a huge possibility. To overcome such a

problem, a high-level security protocol with multiple firewalls must be used like the one used by the US Federal Aviation Administration to protect the landing and taking off of planes.

The final issue is that of consumer awareness. For the past century, the consumer had no role in the cycle; they consume electricity and merely pay the bill at the end of the month. However, with Smart Grids the inclusion of the consumer in the loop is crucial, as they will have the choice of reducing their bill by shifting their use to off-peak hours or choosing what type of energy to use and that will result in the reduction of the peak load consumption and promotion for the use of renewable energy resources [7].

2.3 Renewable Energy Resources

2.3.1 PV penetrated power system

Due to the previously mentioned reasons, it is highly recommended to keep investing and researching about the enhancement of renewable energy's efficiency. However, in this thesis the main concentration will only be on photovoltaic systems. The usage of renewable energy is not a recent trend and solar energy is not an exception. However, it was not till 1954 that Bell labs in the United States came up with the first solar photovoltaic device that can actually produce sufficient amount of electricity. The use of solar energy kept increasing until it finally boomed after the 1970s due to the energy crisis that was going on at the time [8].

Solar panels comprise of semi-conducting materials of both P and N-type. This creates an electric field that directs the electrons from the solar rays that hit the surface and thus creating a current. Unfortunately, a photovoltaic system requires more components that just a solar panel as shown in Figure 2.2. It requires a robust,

steady mounting structure to support the panel at the right angle and through all the changing weather conditions from sandstorms to rain showers. Also, it requires the use of inverters, which are electronic devices that can be used to convert Direct Current (DC) voltage that is generated from the panel to another level of DC voltage or convert the DC voltage to Alternate Current (AC) to be used in the premises or transmitted to the electricity grid. The final component of the system is an energy storage device or a battery. Batteries are not needed if the system is connected to the grid or direct use of generated power for stand alone. Batteries are only needed if the user requires power during the night and the user stores this energy in the batteries during the day for it to be used during the night [9].

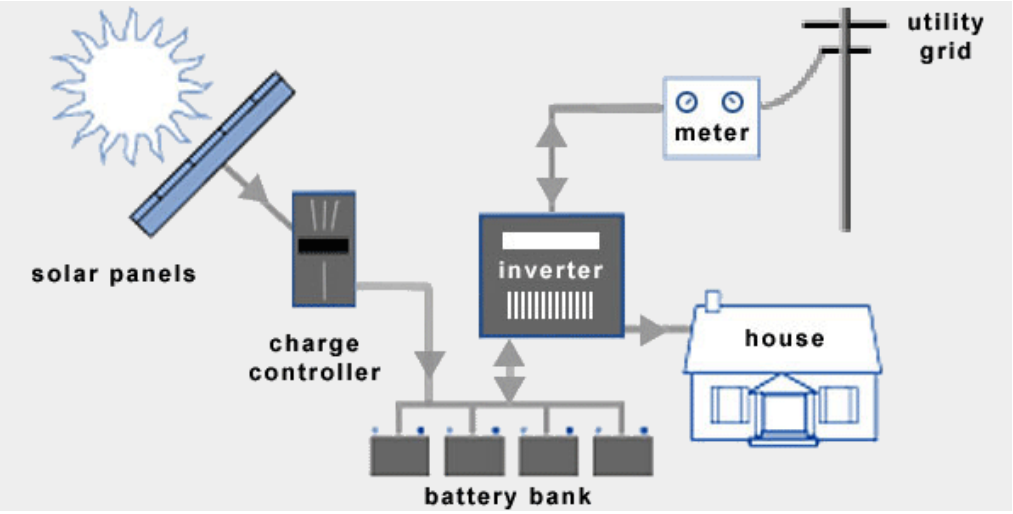

Figure 2.2 PV System Components [10]

Photovoltaic systems have additional advantages that are specific to this type of system. Solar panels have a low operating cost, as it is fully autonomous after installation. They have a low maintenance cost as they are very durable and are designed to operate for a couple of decades. Finally, they are very quiet as they are a static system with no mechanical movement at all [11].

2.3.2 PV Penetrated Power System Challenging Issues

Even though Photovoltaic system is the most widely used type of renewable energy, it still has quite a few downsides that are still under research and enhancement.

2.3.2.1 PV Intermittent Nature

One of the biggest issues with using photovoltaic technology is that it is dependent on weather conditions or to be more specific, on the amount and direction of solar rays reaching the surface of the panel. This makes it highly unpredictable and in some cases unreliable. Another major problem is the percentage efficiency or the conversion rate of the photovoltaic module. Solar panels have one of the least efficiency percentages compared to other energy generating technologies, where the average solar panel converts only 16% into electricity with a range of 12% to 22%. Hence, a large number of panels needed to be installed to compensate for this efficiency. However other electronic devices need to be used such as inverters and energy storage batteries.

The usage of high numbers of solar panels leads to the next problem, which is the area used to install the solar panels and its additional components. Installing solar panels on rooftops is acceptable as it makes use of unutilized areas, however to generate an adequate amount of solar power a vast area of land is needed.

2.3.2.2 Voltage and Control Issues in PV System

Control systems are one of the main regulatory blocks in any modern system and there is no doubt that without these blocks a complex system such as the solar panels will not be able to function. This is demonstrated in Figure 2.3 that shows the basic control objectives in a PV system [12].

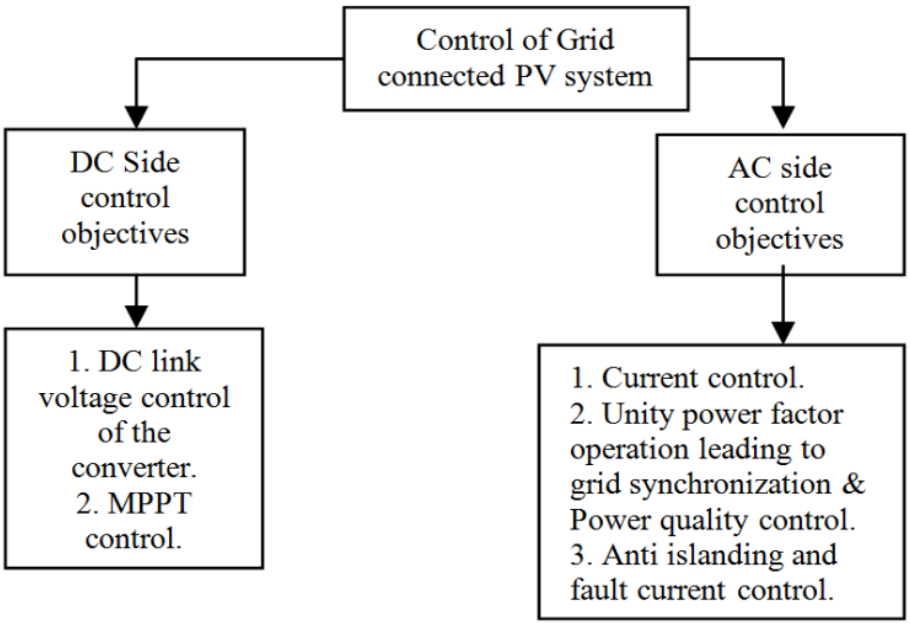

Figure 2.3 PV System Process [12]

Furthermore, there are other operations that control systems are being utilized for, such as identifying faults and malfunctions and dealing with them in a proper manner, so that they do not affect the operation of the rest of the system. Control systems can also be used as an optimization technique that will monitor and regulate the operating temperature to avoid overheating of the panel as high temperature leads to the reduction of efficiency of electronic devices. Moreover, a key use of control is developing an algorithm that determines the optimum operating levels of planning for the production amount needed, the expected amount of solar energy available, and finally how much energy to be delivered or stored. Another aspect is using it for automatic panel wipers. One principle cause of the decrease in the panel's efficiency is all the dust accumulated on the surface of the panel blocking the solar rays from reaching [13].

Implementing the necessary control methodologies solves all the above issues, however, there is a bigger issue that needs to be solved, which is maximizing the

output power problem. Using an MPPT controller, which is discussed in the next section, can solve this issue.

2.3.3 Maximum Power Point Tracking (MPPT)

The MPPT is used to study the naturally low efficiency of the solar cells and seeks to keep the output power as high as possible at all times, especially during varying weather conditions. There are many different MPPT techniques that are used under different circumstances and yield different outputs as well. However, this thesis will focus on three specific techniques: (i) Perturb and Observe; (ii) Incremental Conductance; and (iii) Fuzzy Logic Control. All MPPT techniques are responsible for finding the best and highest combination of the panel's voltage and current to get the optimum level of power.

The voltage versus current of the MPPT graph is presented in Figure 2.4, which shows multiple points including the maximum power point. There are three points that are shown on the curve: point A, B, and C. Point A depicts the power output when using a voltage level of 39 Volts and a current level of 5 Amperes, which produces 195 W of power. Point C has a voltage level of 14 Volts and a current level of 7 Amperes, which produces a power output of 112 W. Points A and C are at the top and bottom of the curve respectively, however, neither of them is the MPP. The MPP is located at the knee point of the curve in between points A and C, which is point B. Point B has a voltage level of 32 Volts and a current level of 7 Amperes, which when multiplied together give a power output of 224 W. Since this is the point where the power output is at its highest, it is called the MPP. Chapter 3 is dedicated to explaining the MPPT and the three control techniques that are used in the design of this Thesis.

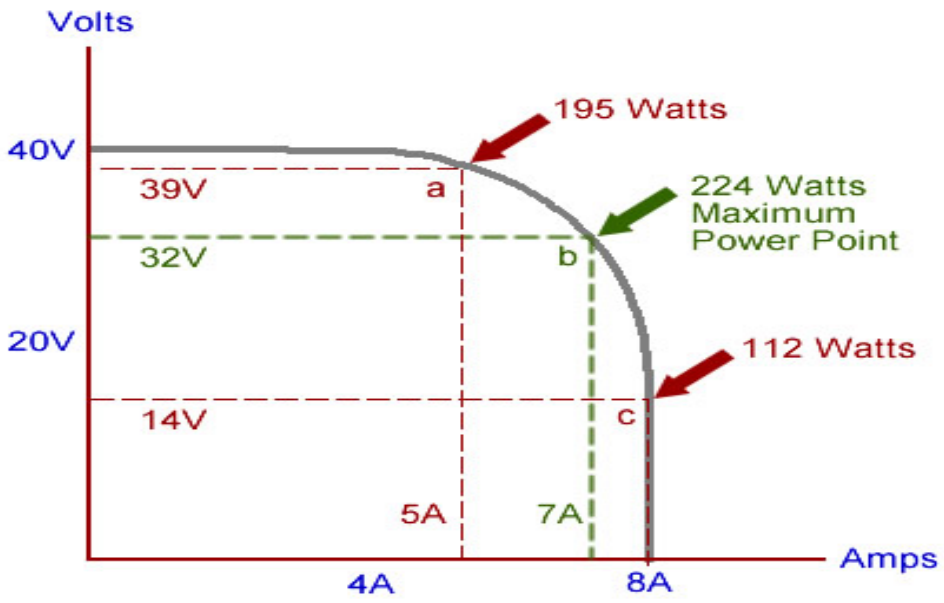

Figure 2.4 Voltage Versus Current of MPPT Graph [14]

2.3.4 Effect of Partial Shading

One issue that affects an MPPT algorithm is partial shading. It is not possible to have a fixed stream of sunlight reaching the surface of the panel. This is due to several reasons such as the changing weather conditions, clouds, unintentional shading and the solar rays' angle of incidence with the panel. Therefore, it is crucial to have an MPPT algorithm to guarantee that the maximum power is being extracted from the solar panel at any given time depending on a particular weather conditions.

Partial shading not only affects the power MPPT curve, it also affects the current vs. voltage curve. To further clarify the effects of partial shading, Figure 2.5 demonstrates both cases of no shading and partial shading side by side. In case of no shading, the power curve has one MPP that is shown by the one peak and there is only one knee point in the current curve, which corresponds to the same voltage level as that of the MPP.

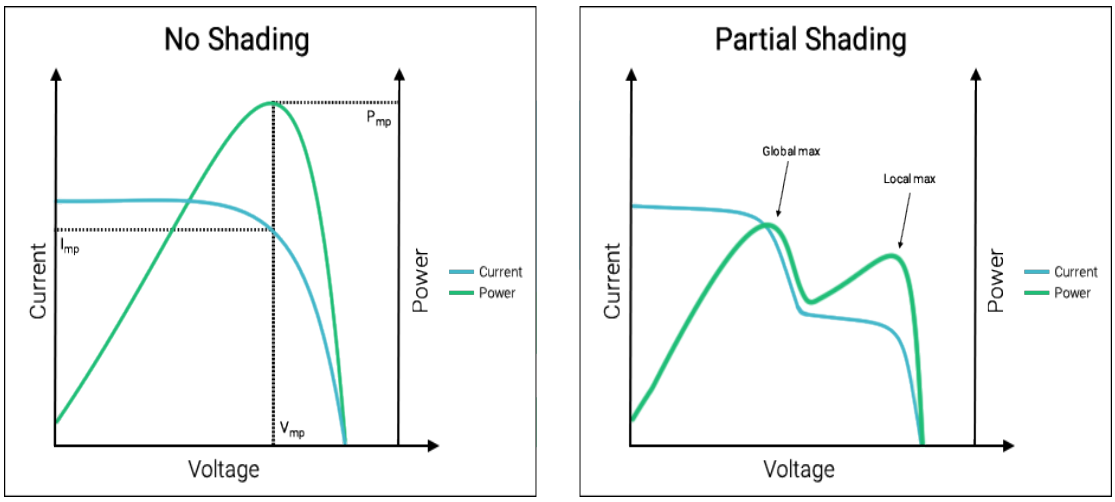

Figure 2.5 Comparison between No and Partial Shading [15]

This power curve is a simplified version of what actually happens in real life as it assumes a constant solar irradiation throughout, which results in having a single MPP in that period. However, due to partial shading the power curve will undergo some changes. In the case of partial shading, multiple peaks can be observed in the power curve that are called local MPP and global MPP and similarly two knee points in the current curve.

Hence, taking into consideration partial shading, the curve will have one or more MPPs, which are called local MPPs but only one global MPP. This is similar to the calculus concept of local maxima and global maxima, where the power curve also has its local MPP peaks and only one global MPP peak as shown in Figure 2.6 below.

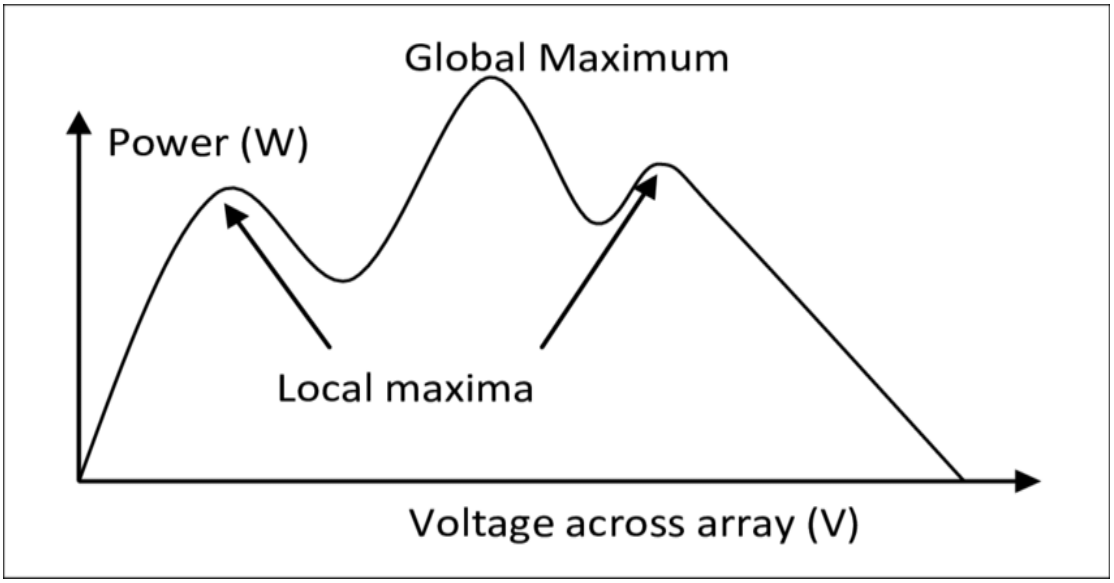

Figure 2.6 Partial Shading Conditions Power Curve [16]

Thus, it is crucial to choose the most suitable MPPT algorithm and match the characteristics of the algorithm to the target goals that are required. Next Chapter explains the three chosen MPPT algorithms thoroughly and discusses their unique features.

Chapter 3 MPPT Controllers

This chapter sheds light on the most common methods and algorithms that are used for MPPT in PV applications. The three types of proposed controllers used are: Perturb & Observe, Incremental Conductance with Integral Regulator, and Fuzzy Logic. As previously mentioned, MPPT techniques are used to ensure the maximization of the system's output power at all times.

3.1 Perturb & Observe Algorithm

3.1.1 Introduction

The first control method used in this thesis is one of the most commonly used in PV MPPT, which is a hill-climbing algorithm called Perturb and Observe (P&O) algorithm. As shown in Figure 3.1, the algorithm's function is to adjust the operating voltage to push the power level to the top of the hill and maintain it there. Figure 3.1 shows a simple power versus voltage MPPT graph under constant conditions, thus not taking into consideration partial shading and its effects as shown in Section 2.3.4.

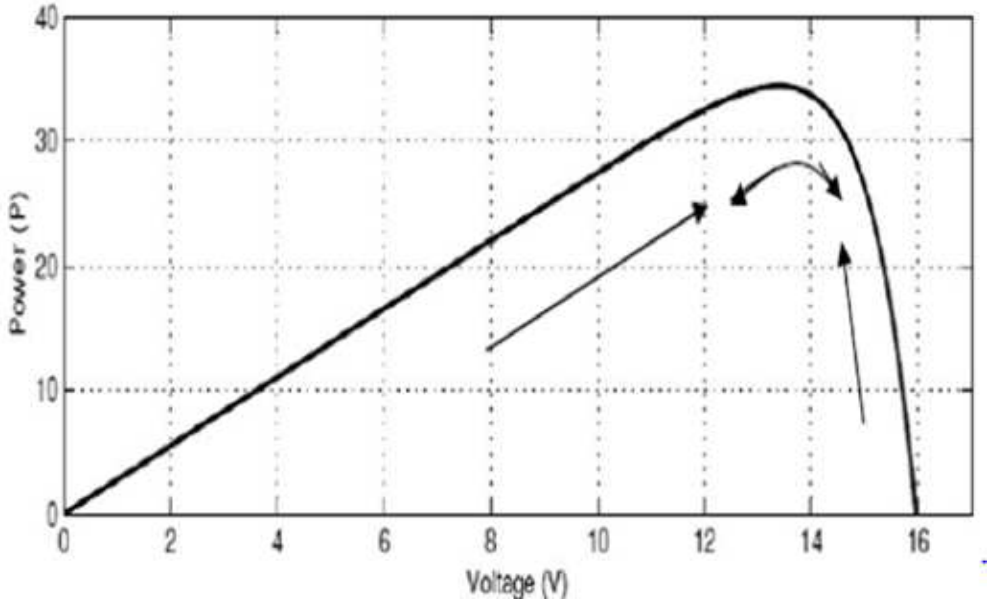

Figure 3.1 Power Versus Voltage Curve Showing P&O's Operation [17]

This method perturbs the voltage and observes the effect that it has on the output power till it reaches the desired point. This is the simplest and easiest method to reach the MPP and is similar to a trial and error method. The algorithm adjusts the operating voltage level by small increments either higher or lower and if the power output increases it continues to do so until the power stabilizes and then stops just before the power starts dropping, which is the knee point in the graph, otherwise known as the MPP. The voltage changes are done through the manipulation of the DC-DC converter's internal resistance by using the Duty Cycle that the MPPT controller outputs as will be discussed later in Chapter 4.

3.1.2 Method of Operation

As previously mentioned, this is one of the simplest methods to implement and only requires a voltage and current sensor to calculate the power and compare it to the previous cycle power. The algorithm's method of operation is presented in the flow chart Figure 3.2.

First, power is calculated using voltage and current and then compared to the previous value of the power. If the difference is equal to zero, then the same voltage will be returned and the algorithm will try to oscillate around the same MPPT. If there is a change in power, the algorithm will then go forward and check the difference in voltage levels. In the case of a positive power difference, the algorithm will notice and direct the voltage to the same direction (increase or decrease) as the previous case. Hence, if the voltage difference is positive then the algorithm will keep increasing the voltage and vice versa. However, in the case of negative power difference, the algorithm will do the complete opposite and will direct the voltage to the other direction. This means that if the voltage change is negative then the algorithm will increase the voltage and finally if the change in voltage is positive the

algorithm will decrease the voltage. Thus, the four cases that the algorithm is required to evaluate and react to are as follows:

1. $\Delta P > 0$ and $\Delta V > 0$ → Increase the voltage.
2. $\Delta P > 0$ and $\Delta V < 0$ → Decrease the voltage.
3. $\Delta P < 0$ and $\Delta V > 0$ → Decrease the voltage.
4. $\Delta P < 0$ and $\Delta V < 0$ → Increase the voltage.

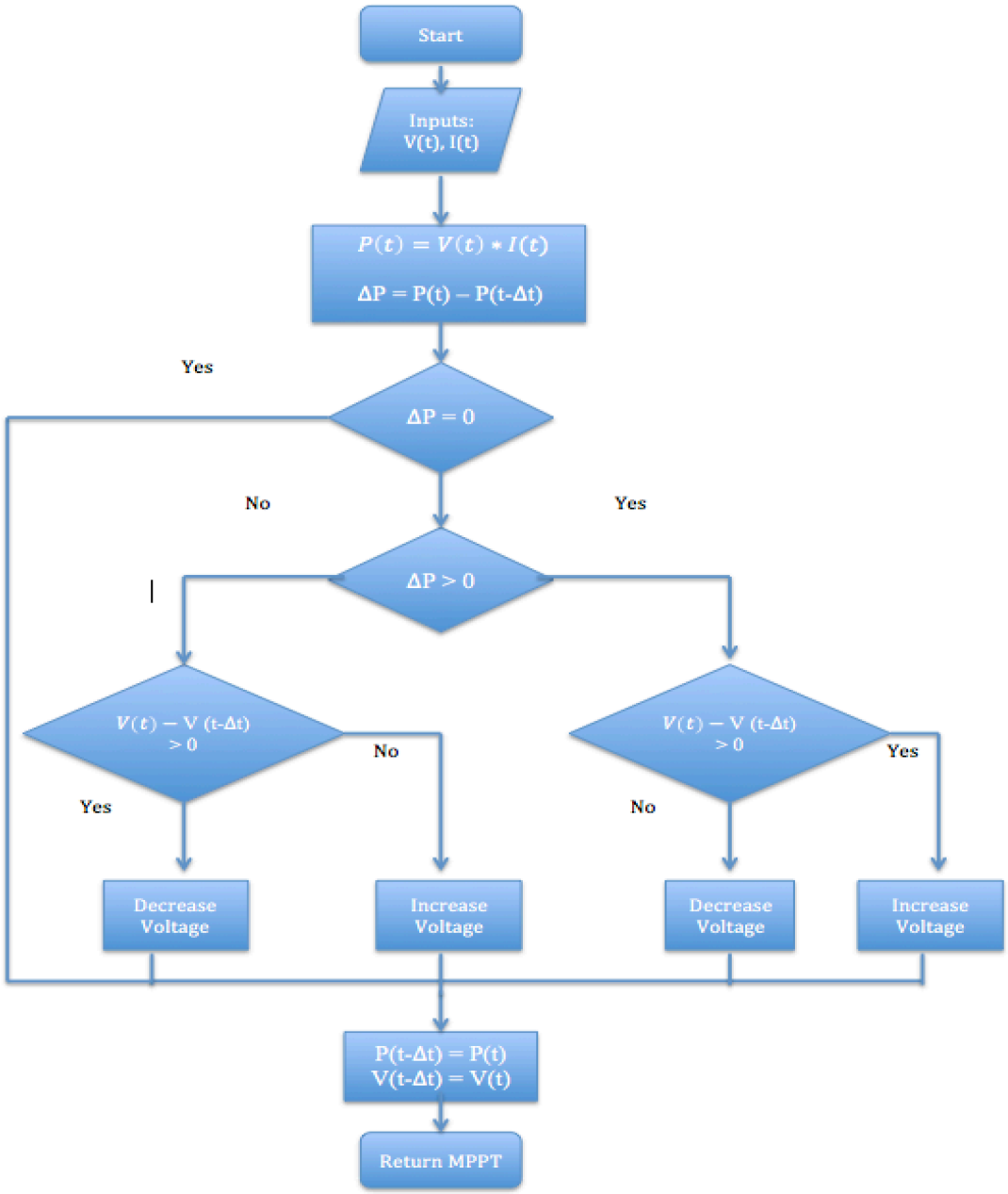

Figure 3.2 Perturb and Observe Flow Chart [18]

The algorithm can manipulate the operating voltage freely by varying the duty cycle ratio. Any change in the duty cycle will consequently have an inverse effect on the input resistance of the DC/DC converter and thus will alter the operating voltage to satisfy the four cases mentioned above [19]. Table 3.1 illustrates the relationship between the duty cycle, input resistance, output power, and the voltage in the next cycle as shown below.

Table 3.1 Effect of Duty Cycle on Input Resistance, Output Power, and the Next Cycle's Voltage

Change in Duty Cycle	Change in Input Resistance	Effect on Output Power	Next Cycle's Voltage Change
Increase	Decrease	Increase	Decrease
Increase	Decrease	Decrease	Increase
Decrease	Increase	Increase	Increase
Decrease	Increase	Decrease	Decrease

As shown in Table 3.1, any change in the duty cycle will have an inverse effect on the input resistance of the converter and hence have an inverse effect on the operating voltage. The algorithm then observes the effect of that change in the duty cycle on the output power to calculate the right command in the next cycle. The output power can increase or decrease depending on whether the current operating voltage level is before or after the knee point in the power graph as shown in Figure 3.1. If the operating level is beyond the knee point or the MPP, then an increase in the voltage will decrease the output power and vice versa. For example, in the third case in Table 3.1, a decrease in the duty cycle causes an increase in input resistance or operating voltage and results in an increase in the output power. This means that the current operating level is before the MPP and by increasing the voltage the output power will increase and thus in the next duty cycle the algorithm will opt to increase the voltage which can be achieved by reducing the duty cycle.

3.1.3 Advantages and disadvantages of P&O method

Perturb and Observe method is a widely known hill-climbing method for several reasons. Firstly, it is the most simplistic algorithm for MPPT and only requires one voltage sensor. For that reason, it is a fast, inexpensive, and easy to implement option. Secondly, unlike the other MPPT algorithms that will be discussed further on, P&O method has a short computing time and a low computing complexity as it does not require any mathematical calculations. Only a comparison of the current and previous voltage and power values is required. This enables P&O to decide which side the current level is on with respect to the knee point and to move the voltage in the correct direction swiftly. However, this simplistic approach has its failures especially when dealing with a complex system such as a PV array. The first downside to this algorithm is that, given its method of operation, the voltage level never stays in the same level even when the MPP is reached similar to the power level. The algorithm cannot help but continue to perturb. Once it reaches around the MPP it decreases the perturb magnitude but that still causes significant power loss compared to the other algorithms. Another disadvantage of using P&O is the way it responds to the continuously changing weather conditions [20]. As the weather changes and the irradiance hitting the panel's surface increases, the MPP automatically shifts to the right as shown in Figure 3.3.

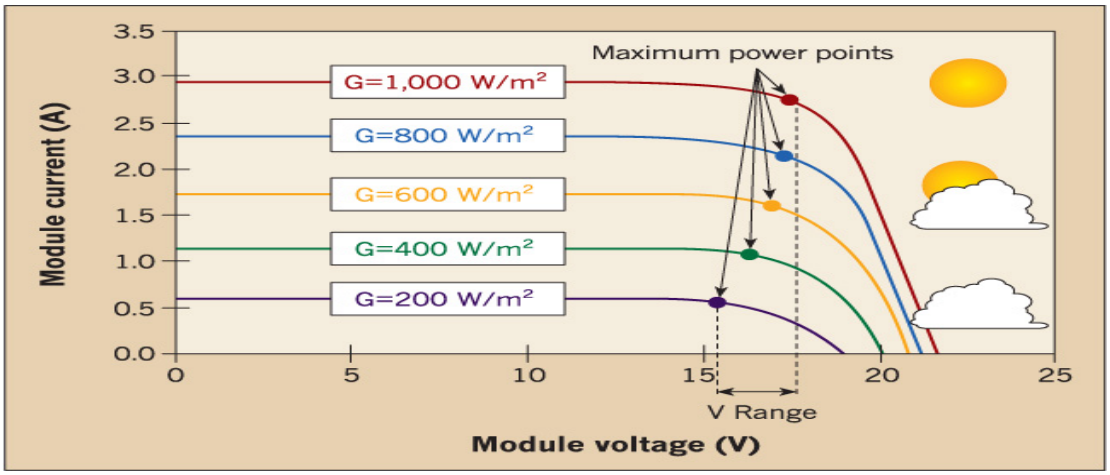

Figure 3.3 MPP Voltage Shift when Varying the Irradiance [21]

The difference in the voltage level between the 200-W per square meter and the 1,000-W per square meter irradiance is not very high, but is high enough to trick the algorithm. Once the MPP shifts to the right or gets further away from the algorithm's point of view, it understands it as a change due to the perturb and will automatically cause the next cycle to move in the other direction which is in fact the wrong direction and it is moving away from the MPP.

3.2 MPPT using Incremental Conductance (INC)

3.2.1 Introduction

Among the many different algorithms that are utilized to achieve MPPT, one of which is Incremental Conductance (INC). INC is another hill-climbing MPPT algorithm such as P&O; however, it operates in a completely different manner than P&O. INC exploits the power curve as shown below in Figure 3.4 to calculate and track the maximum power point. The simplified power diagram in Figure 3.4 will be thoroughly explained in this chapter to demonstrate how INC operates.

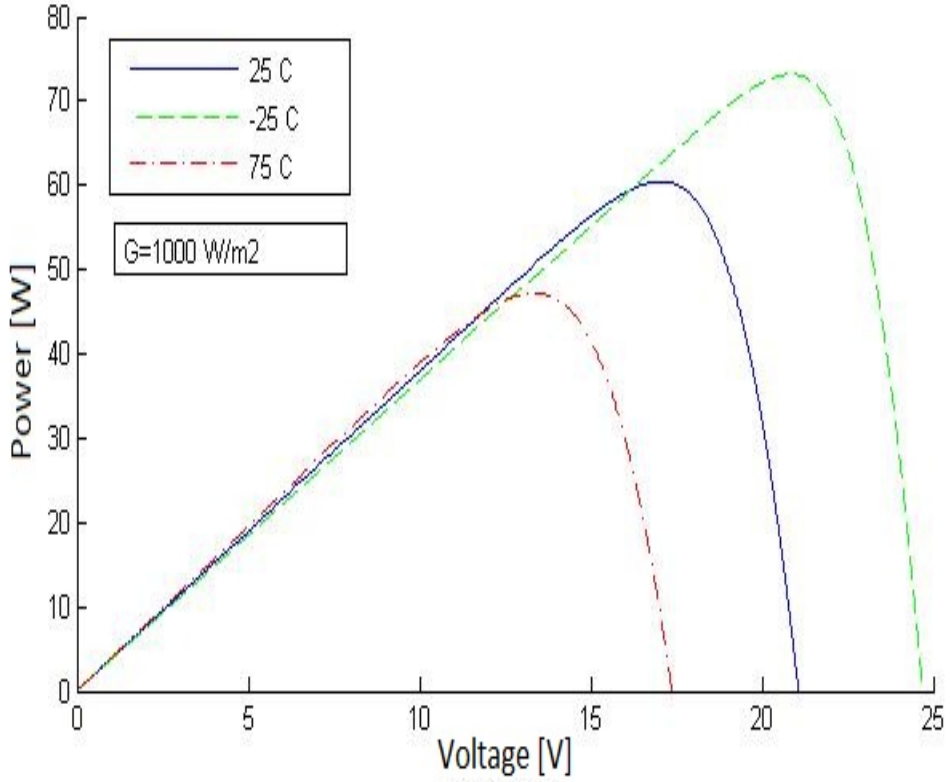

Figure 3.4 Power Versus Voltage Curve under Varying Temperature [22]

In Figure 3.4, the solar irradiance is kept constant at a rate of 1000w/m2 and the effects of the temperature changes on the output power are monitored. The MPP can be achieved when the slope of the curve is exactly zero: positive before that point and negative after that. Thus, using the above graph at temperature 25 ℃, the MPP is the point where dP/dV = 0 and that is located at 18V approximately. Similarly, by viewing the I-V curve for the same model as shown below in Figure 3.5, the Maximum Power Point can be located when the sum of the instantaneous conductance (which is Ipv/Vpv) and the incremental conductance (which is the derivative of the instantaneous conductance) are equal to zero.

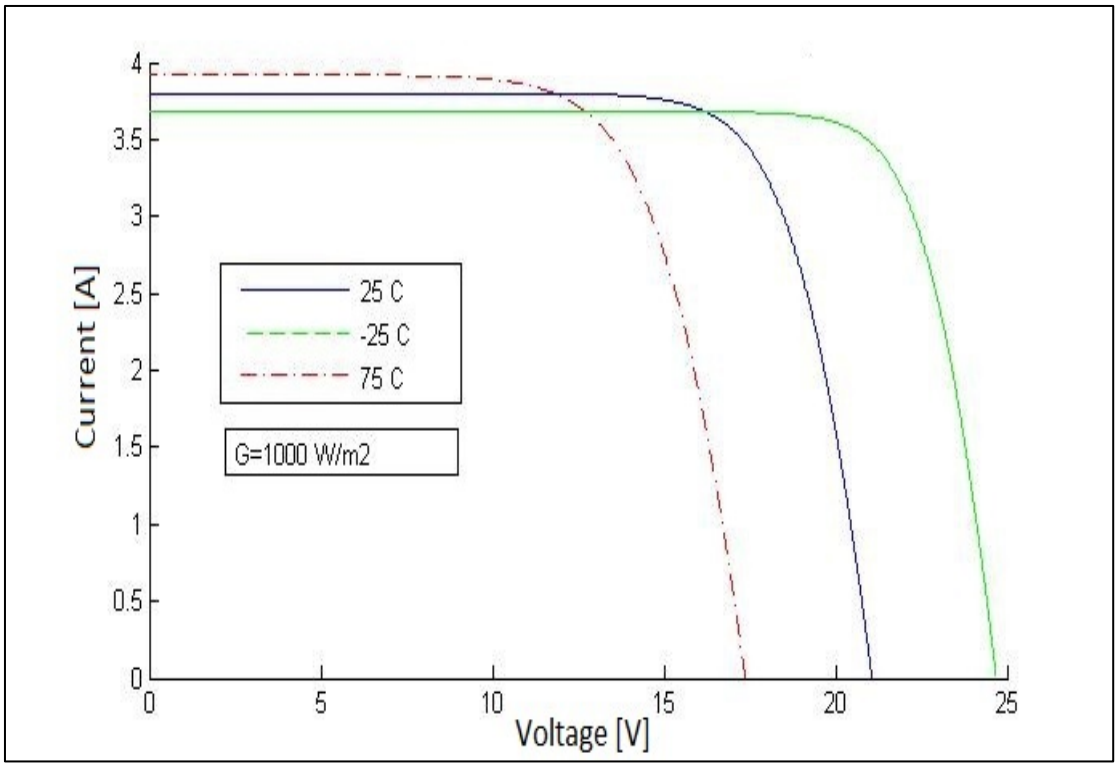

Figure 3.5 Current Versus Voltage under Varying Temperature [22]

Thus, the three stages of the MPPT curve are as follows [23]:

1. Pre-MPP: dP/dV and the sum of the instantaneous and incremental conductance (Ipv/Vpv + dIpv/dVpv) are both positive.
2. At the MPP: dP/dV and the sum of the instantaneous and incremental conductance are both equal to zero
3. Post-MPP: dP/dV and the sum of the instantaneous and incremental conductance are both negative.

3.2.2 Method of Operation

This section of the chapter intends to clarify the incremental conductance algorithm through the use of a flow chart. In order to do that, further analysis of the three stages of the MPPT curve is required. Section 3.2.1 presented the method for identifying the MPP. Moreover, some mathematical tweaking needs to be done on those rules to

understand what gets fed into the MPPT controller. As previously mentioned, there are three stages in the curve:

1. Pre- MPP: dP/dV is positive.
2. At the MPP: dP/dV is equal to zero
3. Post MPP: dP/dV is negative.

Since P = IV, thus $dP/dV = dI*V/dV.$ (3.1)

Equation 3.1 leads to:

$$(V* dI/dV) + I \quad (3.2)$$

Further manipulation will result in:

$$dI/dV = -I/V \quad (3.3)$$

Thus, applying equation 3.3 on the three stages results in:

1. Pre- MPP: $dI/dV > -I/V$
2. At the MPP: $dI/dV = -I/V$
3. Post MPP: $dI/dV < -I/V$

The above calculations are meant to provide an understanding of the algorithm's inputs at the sensor level of the circuit. It demonstrates that in order for the algorithm to locate the MPP, it compares the values of the change in I/V with -I/V until both are equal and that is when it reaches the MPP.

After clarifying the inputs of the algorithm and how they are utilized, the next step is mapping out the flow chart of the algorithm's cycle. The flowchart in Figure 3.6 shows the sequence of steps for the algorithm.

The starting point of the flowchart is to input the values of both the current and the voltage outputs of the PV array. The step of updating the voltage and current of the PV array is done intermittently depending on the chosen duty cycle. As soon as the controller receives these inputs, it evaluates and compares them with the previous

input values. The subsequent steps will vary depending on the input values; however, the following points are what the algorithm is evaluating:

- The change in voltage
- The change in current (>, <, or = 0)
- Change in $\frac{I}{V}$ compared to $\frac{-I}{V}$ (>, <, or = 0)

Depending on the points to be evaluated, the controller will keep adjusting the voltage level to return the MPP based on the conditions stated in the beginning of Section 3.2.2.

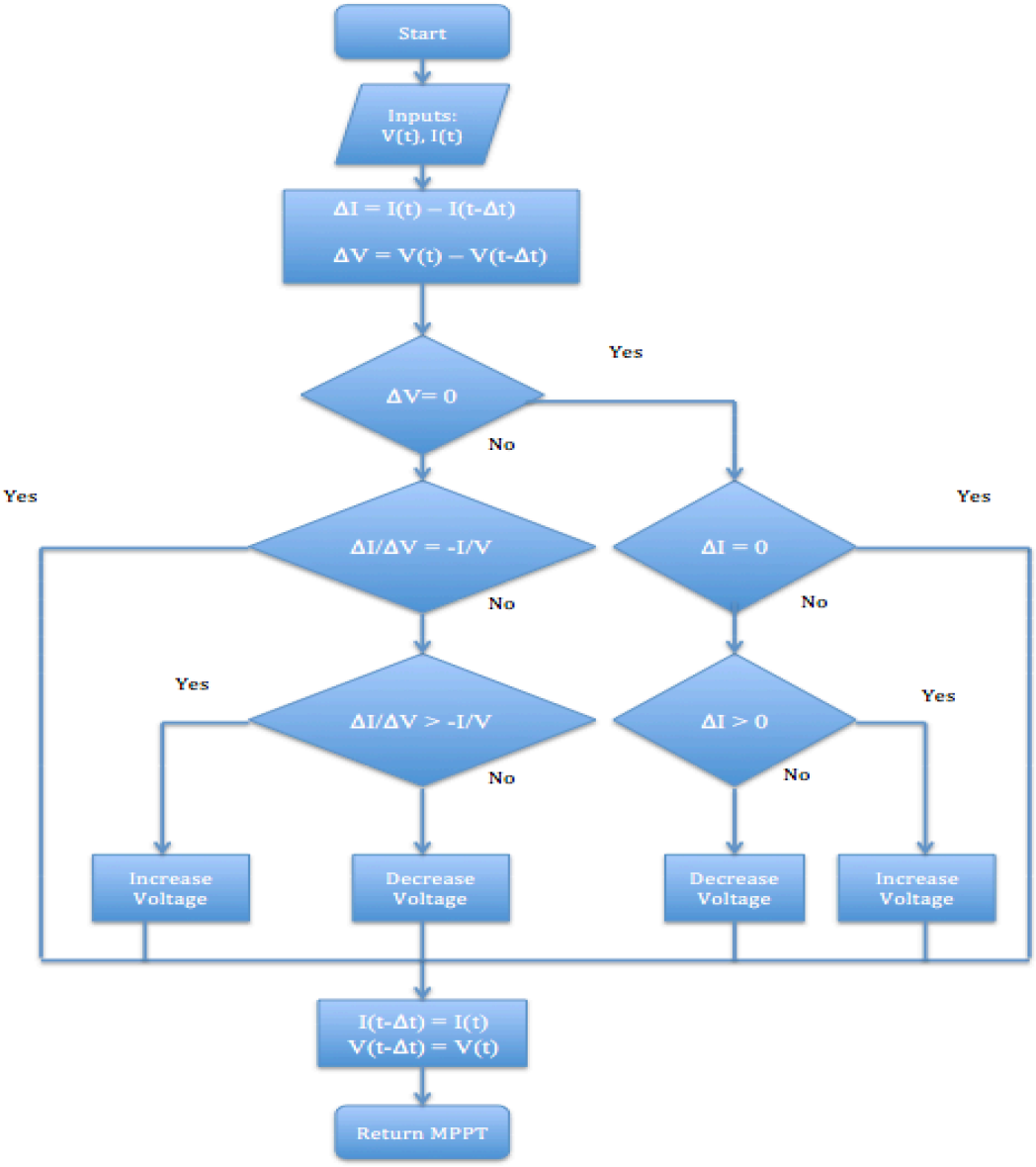

Figure 3.6 INC Algorithm Flowchart [23]

3.2.3 Advantages and Disadvantages of INC

Incremental conductance is one of the commonly used hill-climbing algorithms in MPPT controller and there are several reasons behind that. First and foremost is the method of tracking the MPP. As discussed in the previous sections, INC has successfully divided the PV power output graph into three sections Pre-MPP, MPP and Post-MPP. Each of these sections has a unique value for dP/dV: positive, zero, and negative. Thus by exploiting these facts, INC has a clear advantage over the P&O algorithm, which is the computational time and accuracy of the MPP. During changing weather conditions, the P&O method will keep on oscillating to get close and locate the MPP. However, using INC, no oscillations are required and the algorithm knows exactly which stage of the previously mentioned three it is in and will increment or decrement the voltage immediately until it reaches the zero slope, which is the MPP and thus, the computational time is reduced. Another advantage is the higher accuracy when it comes to tracking MPP. Unlike P&O that oscillates around the MPP, INC is able to pinpoint the location of the MPP, which means it has a higher efficiency. The two downsides of using INC are the complexity and the possible inaccuracy. Even though INC is much less complex than Fuzzy logic, it is still more complex to implement than P&O. Furthermore, when it comes to MPPT it is not the best algorithm to be used but it is superior to that of the P&O. When it comes to choosing which algorithm to be used for MPPT, there is always a tradeoff, speed and efficiency on one hand and complexity and price on the other one.

3.2.4 INC Coupled with Integral Regulator (IR)

The target of the MPPT is to track and locate the global MPP since it has the highest efficiency. However most tracking techniques might mistake the local MPP with a

global MPP and thus it will take longer to track and it might need more advanced algorithms for better tracking of the global MPP.

To combat both the efficiency concern and to try and reduce the time needed to locate the global maximum, an integral regulator was used along with the incremental conductance algorithm as shown in Figure 3.7. This figure illustrates that the addition of the integral regulator adds an extra step between the MPPT algorithm and the PWM generator. The integral regulator is used to increase the output efficiency by performing duty cycle correction. This allows for more control, grip, and adaptation with the ever-changing weather conditions that affect the MPP and hence increase the system efficiency.

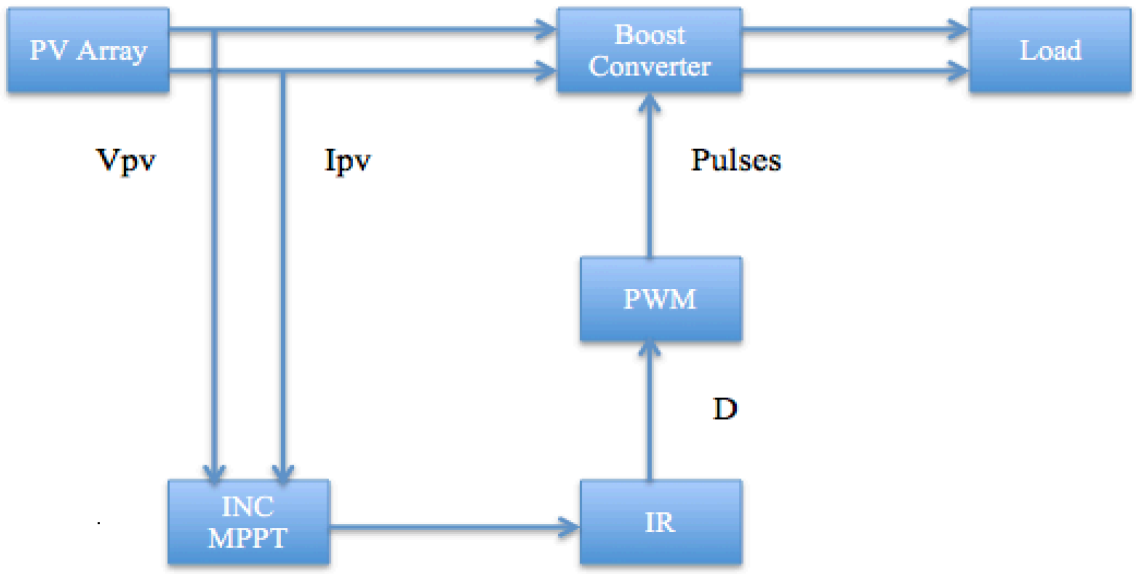

Figure 3.7 MPPT with Integral Regulator

This adaptive method increases the system efficiency using three key factors. Firstly, the IR improves the method of operation of the incremental conductance by reducing the error between the instantaneous conductance and the incremental conductance (as discussed in Section 3.2.1). Secondly, as another hill-climbing method like the P&O

algorithm, the INC suffers from constant oscillations or ripples in the output. Adding the integral regulator can reduce these ripples, which will also result in a better digital resolution of the output. Lastly, the integral regulator improves the accuracy of both the system's large step sizes for when the operating level is far from the MPP and also the small step sizes when the MPP is reached to extract the highest possible level of power [24].

3.3 MPPT Using Fuzzy Logic Controller

3.3.1 Introduction to Fuzzy Logic

Fuzzy logic is considered a type of many-valued logic (MVL) or otherwise called non-classical logic. They are a form of logic that do not constrain the output truth-values to only two but accept the range of values in between as well [25]. This means that it not restricted to binary values of "0" and "1" or "True" and "False", but operates as well in the grey area in between allowing for a more accurate indication of the variable. Another unique attribute that fuzzy logic has is the use of linguistic interpretation instead of numerical, which makes it closer to the human thought process. When Lukasiewicz and Tarski introduced infinite-valued logic in 1920 and when Lotfi Zadeh perfected it and introduced fuzzy Logic in 1965, they all knew that a new framework that is not only black and white was needed [26].

3.3.2 Fuzzy Sets and Membership Functions

Fuzzy logic is a unique method that transforms mathematical equations into a set of linguistic commands which is done using two crucial aspects: fuzzy sets and membership functions. Fuzzy sets are a group of sets where the numerical data gets allocated to, and by doing so it transforms numerical values into linguistic ones. Fuzzy sets are similar to the Mathematical concept of having a universe of discourse,

where a universe defined as Z contains all the values and the data are grouped. A simple example of a fuzzy set would be creating three sets called low, medium, and high, used to divide and group the available numerical data into these sets using the second concept, which is the membership function. The membership function is a tool developed through the experience of the user and is used to assess the degree to which this value belongs to a certain set and is evaluated on a scale of zero to one. As shown in Figure 3.8, the triangle shape represents the membership function which is bound by zero and one, where zero means that the variable does not belong to the set at all and one means that it the variable entirely belongs to the set.

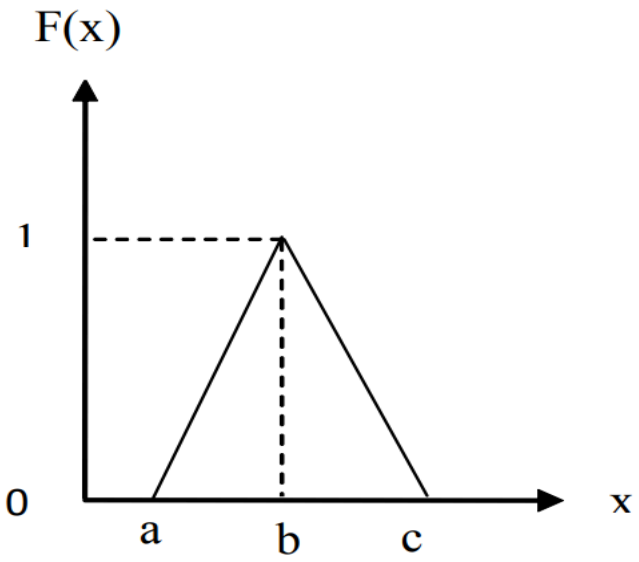

Figure 3.8 Membership Function Diagram [27]

Each fuzzy set is represented by a triangle or a membership function, thus the more sets the system has the more triangles there will be. Figure 3.9 shows how the graph looks like with three sets of low, medium, and high for a certain variable. There are two points that stand out in Figure 3.9; the first is the shape of the membership functions and the second is the overlapping of the functions. It is quite common to have a trapezoid as a membership function and not a triangle. This depends on the

range of variables the user has deemed to have a degree one membership value. So, the triangle is a special case of the trapezoid where there is only one measured variable that has a membership value of one.

The other point worth discussing is the overlapping of the functions. Since the membership value given to each of the input variables is not always a binary value and the input variable can have a membership value for more than one set, it is normal to have an intersection area between the two functions. The x-axis of the area of intersection represents all the measured variables that are not purely valued in one set and have a value in both sets. The way to identify the membership value for a variable is to move upward along the y-axis of that variable and notice where that line intersects with one or more functions. To further clarify, using the previous example with the three sets of low, medium, and high, and assuming an x-axis range from zero to ten: if the measured variable to be assessed was the number eight then the result will be that the number eight has a membership value of 0.6 for the high set and a value of 0.4 for the medium one.

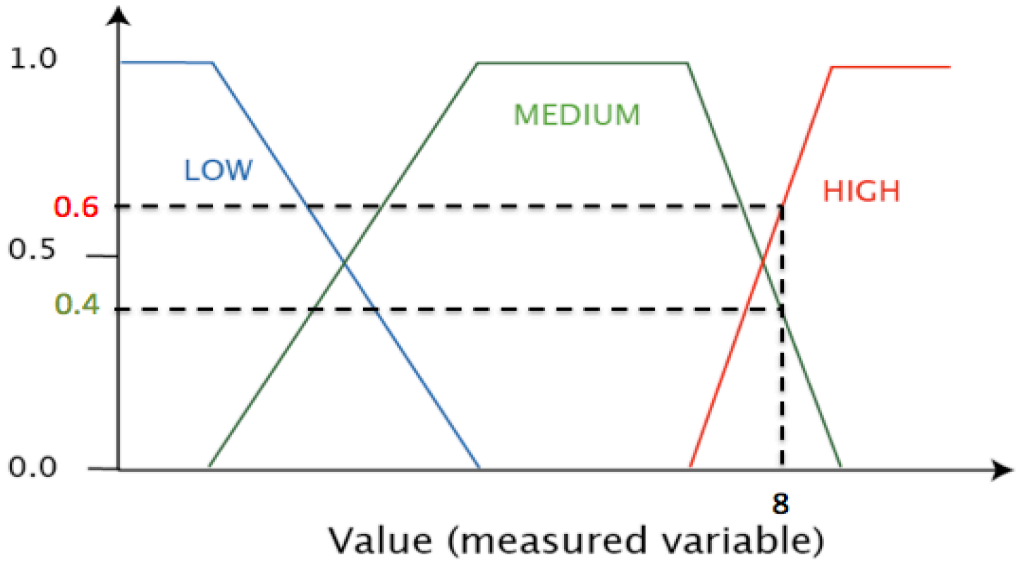

Figure 3.9 Fuzzy Set that Includes Three Membership Functions. (Adapted from [28])

3.3.3 Fuzzy Rules and Reasoning

A fuzzy set can be adapted and tailored towards any application and that is due to the fuzzy rules that are embedded in each of the sets. A fuzzy rule is a statement developed by the user of the logic based on the knowledge of the industry experts to determine the output based on the input variables. These rules are formulated as conditional statements that utilize the "if" and "then" arguments along with some logic gates as well such as "and", "not" and "or" [29]. The rules were built in such a way to mimic the day-to-day human reasoning that is being done naturally such as "IF room temperature is *low* THEN switch the air-conditioning to *low*." In this conditioning statement, the "if" and "then" argument was used to figure out the output and input. In this case, the output is the air-conditioning fan level and the input is the room temperature. The final elements of the rule are the fuzzy sets that represent both the input and the output values, which in this case are both called low. A general fuzzy rule should look like equation 3.4:

$$\text{IF X is } FS \text{ THEN Y is } FS \tag{3.4}$$

Where:

X is the input measured variable.

FS is the Fuzzy Set assigned to each variable.

Y is the output measured variable.

Equation 3.4 is the most general and simplified version of the fuzzy rule but as the application gets more and more complicated slight changes can be noticed on the rule such as the number of inputs, the number of outputs, and finally the number of conditions in the rule.

Now that the fuzzy rules have been explained, the next part is to understand how the user programs the set of fuzzy rules so that fuzzy logic can calculate the output from

the value of the input variables. Figure 3.10 is what a typical set of fuzzy rules look like once the user has programmed it. The figure shows the nine rules of the fuzzy rule design of a nonlinear process that has three membership functions, two input variables and one output [30]. There are two input variables, which are the error signal and the change in the error signal. Secondly, the three membership functions represent the variables that have been transformed from numerical to linguistic state. The three membership functions are N, Z, and P respectively, which as stated in the figure refer to negative, zero, and positive. Finally, three different values, which are small, medium, and big, or S, M, and B can denote the output respectively. The output can be calculated by figuring out the intersection point between the two inputs or the intersection of the rows and columns. For example, if the input error signal is a negative number and the change in the error is zero then the intersection point would be M, which means the output would be a medium number.

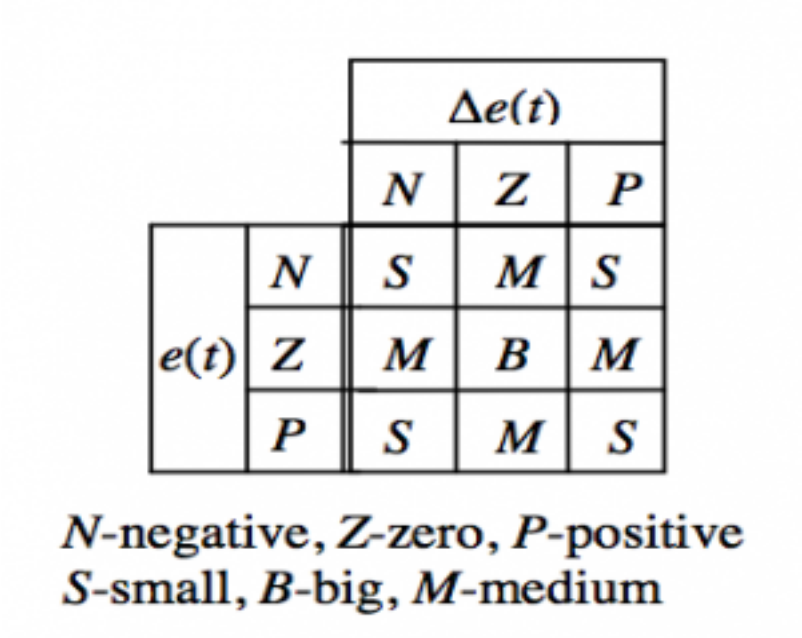

Figure 3.10 Fuzzy Rules [30]

3.3.4 Fuzzy Logic Controller

In this section, the full method that the fuzzy logic controllers utilize is comprehensively explained. There are four fundamental stages that occur in any fuzzy logic controller and they happen in the following order:

1. Fuzzification
2. Knowledge or rule base
3. Inference engine
4. De-fuzzification.

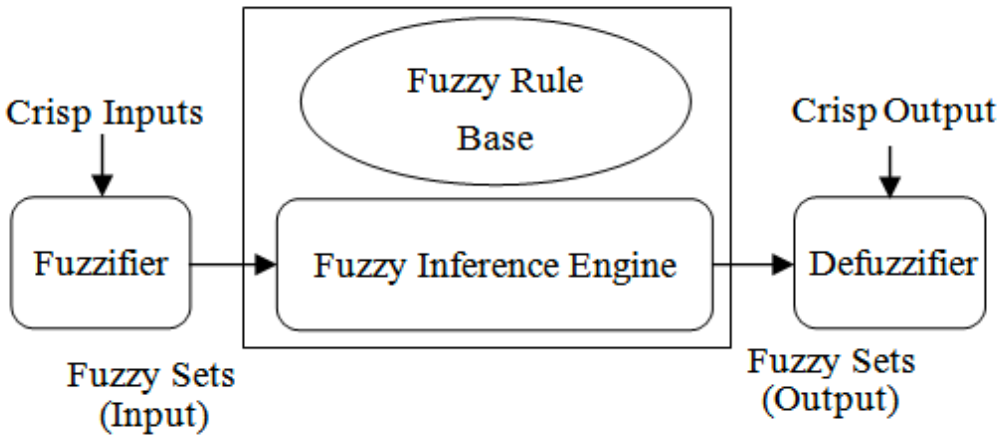

Figure 3.11 Fuzzy Logic Process [31]

The fuzzification process is shown in Figure 3.11. The fuzzifier is being fed crisp inputs, which are the input variables in their numerical or analog forms. As soon the fuzzifier receives those input variables, it evaluates them to figure out the fuzzy set that it belongs to. Finally, the fuzzifier transfers the numerical value into the linguistic value that is equivalent to the label of the fuzzy set it belongs to.

The second stage of the fuzzy logic controller is the knowledge or the rule base. This is where the user adds his expertise and the knowledge required to form the fuzzy

rules. Not only does this base translate the user's experience into the fuzzy rules but also forms the control goals and policies of the user.

The third stage of the controller is the fuzzy inference engine, which is responsible for the decision-making action. The fuzzy inference engine receives the input from the fuzzifier and at the same time extracts the knowledge from the rule base to come up with an output that matches the users policies. Once a decision has been made and the engine calculates the output, it then pushes it to the last part of the controller, which is the de-fuzzifier. The de-fuzzifier, as the name suggests, does the complete opposite of the fuzzifier. It receives the output from the fuzzy inference engine in the form of a fuzzy set label and then proceeds to transform this output from linguistic form into numerical or crisp form [32].

3.3.5 Method of Operation

Figure 3.12 describes the method of operation of a fuzzy logic controller through the use of a flowchart. The controller starts by setting an initial value for the duty cycle and then measures the values of both the PV output voltage and current. The PV output voltage and current values are then used as input signals to the FLC MPPT controller to calculate the power output.

Furthermore, the measured value of the voltage along with the calculated value of the power are used to calculate the value of the error and the change in error between the inputs of the current and previous cycles. The error signal is the instantaneous error that is calculated using equation 3.5 and this error signal goes to zero when the algorithm reaches the MPP.

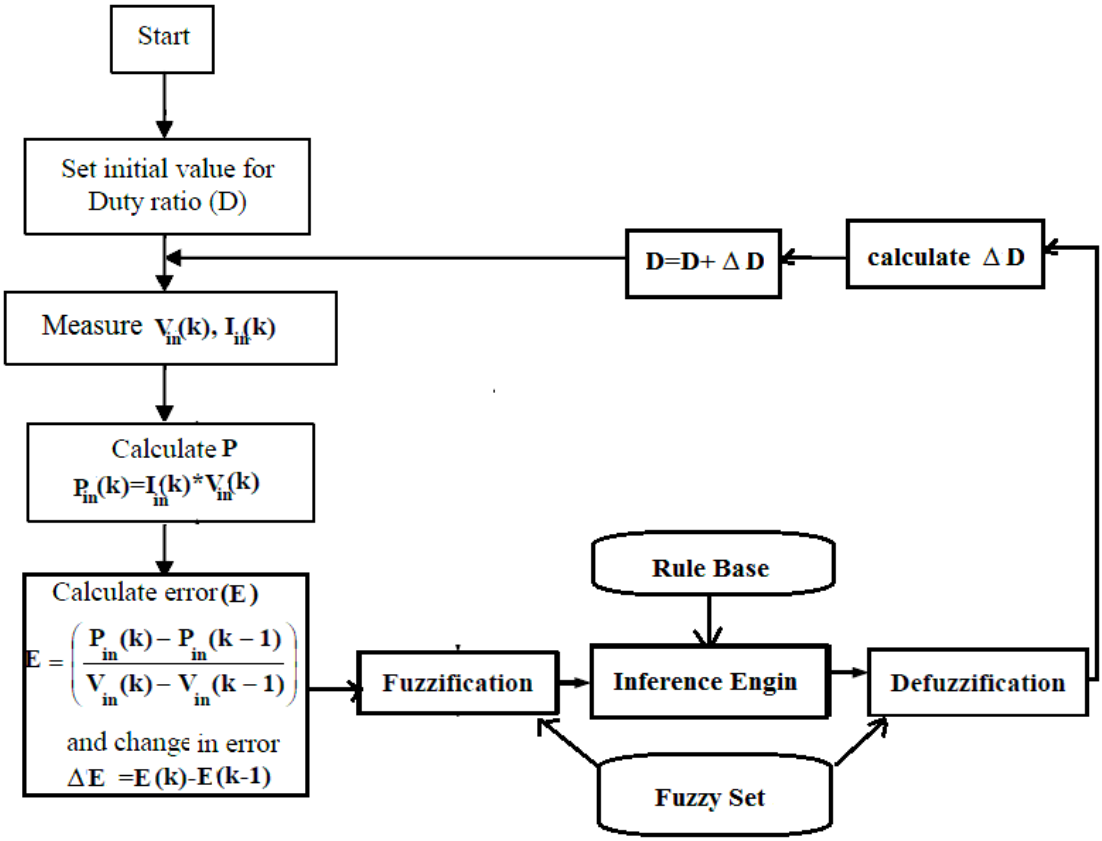

Figure 3.12 FLC Design Flowchart [33]

Both the error and the change in error can be calculated by using Equations 3.5 and 3.6 shown below:

$$E(k) = \left(\frac{Pin(k)-Pin(k-1)}{Vin(k)-Vin(k-1)}\right) \tag{3.5}$$

Where:

E(k) is the error signal value

Pin(k) is the current cycle's power value

Pin(k-1) is the previous cycle's power value

Vin(k) is the current cycle's voltage value

Vin(k-1) is the previous cycle's voltage value

$$\Delta E = E(k) - E(k-1) \tag{3.6}$$

Where:

E(k) is the current cycle's error signal value
E(k-1) is the previous cycle's error signal value

Once the error and the change in the error values are calculated, the fuzzy logic process described in Section 3.3.4 starts. The controller takes these two values in as crisp inputs and changes them into linguistic values corresponding to their fuzzy set label, which is the fuzzification process. The inference engine in the controller then calculates the output decision based on the inputs it receives from the fuzzifier and the fuzzy rules the user has installed in the knowledge base. The de-fuzzifier then transforms the received output decision from linguistic to numerical or crisp value. This numerical value is the change in the duty cycle required to have the output at the MPP. Thus, the new duty cycle is equivalent to the old duty cycle plus the change in duty cycle calculated. The change in duty cycle can be either positive or negative depending on the required final duty cycle as shown in Equation 3.7:

$$D(k) = D(k-1) + \Delta D \tag{3.7}$$

Where:

D(k) is the new cycle's duty cycle ratio ($0 \leq D(k) \leq 1$)
D(k-1) is the previous cycle's error signal value
ΔD is the calculated change required in duty cycle ($-1 \leq \Delta D \leq 1$)

3.3.6 Advantages and Disadvantages of Fuzzy Logic

The popularity and usage of fuzzy logic have been increasing steadily ever since Zadeh created it in 1965. This section clarifies this usage by presenting the advantages and drawbacks of fuzzy logic control.

There are numerous advantages for using fuzzy; however the main one that stands out is the user-friendly logic. The concept that fuzzy logic was built on was to mimic the human thinking process, which is why fuzzy logic transforms numbers into language and the rule base is configured by sentences instead of mathematical equations. Thus, making it not only much more convenient for the users but also faster to program. Another major advantage is that unlike other controllers, fuzzy logic has the ability to work with imprecise mathematical models or ones that are approximated and still provide an efficient output. Fuzzy logic is consistent and robust even during frequently fluctuating applications such as the weather condition with solar panels. Finally, fuzzy logic is capable of working in parallel with other control techniques such as PID or state feedback [34].

On the other hand, like any other control technique, fuzzy has its drawbacks. Firstly, compared to P&O and INC, FLC is much more complex. The former two techniques require the usage of one or more sensors and thus they are simpler to use. Moreover, higher complexity translates into higher cost of implementation. Another drawback is when an accurate mathematical model of a complex project is available; it tends to be easier and quicker to use a controller that utilizes this model instead of re-writing the model to conditional statements. In this case fuzzy would not be the optimum choice.

Chapter 4 Design & Analysis

4.1 Introduction

This chapter presents the Thesis design of the solar PV system with MPPT controller integration. There are two types of solar PV systems: standalone and grid-connected. In this Thesis, the standalone system is chosen because the focus is on the generation of the supply side and how to enhance it rather than the demand or load side. The four main components of any PV architecture are: solar panel array, MPPT controller, converter, and finally the load. The system is shown in Figure 4.1 below.

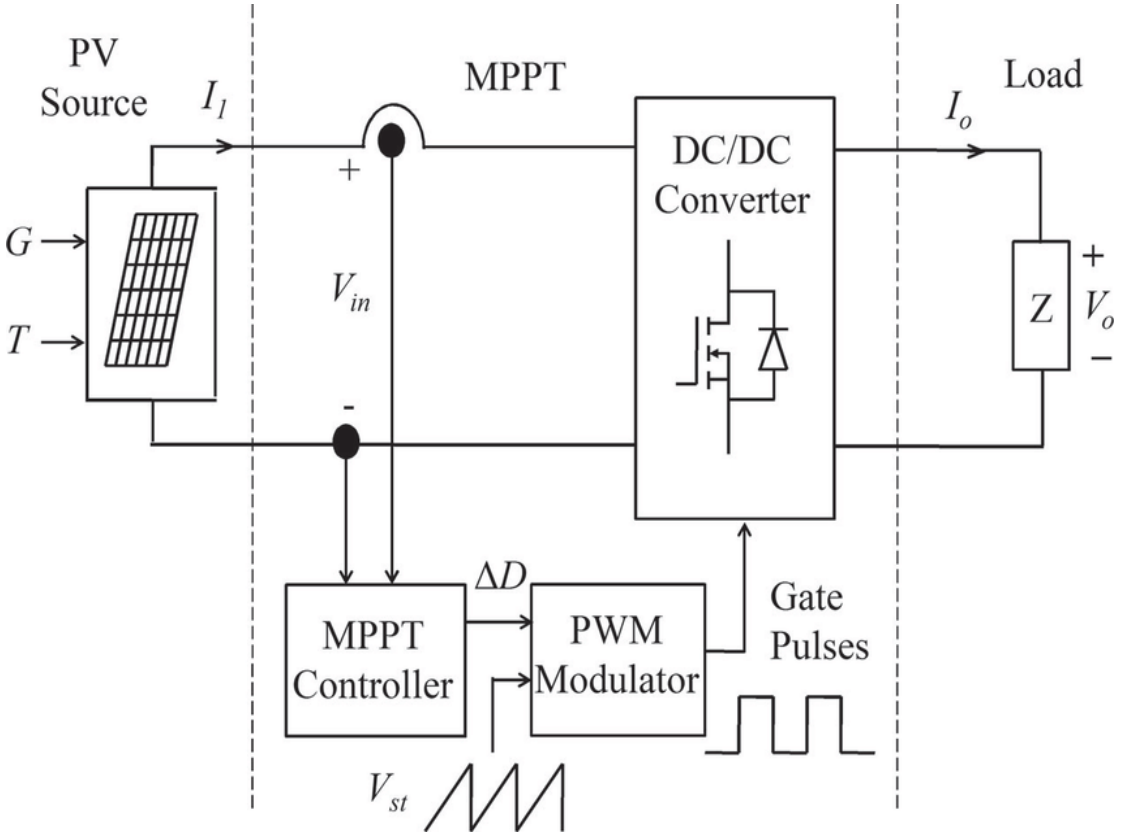

Figure 4.1 Solar PV System with MPPT Controller [35]

4.2 System Architecture

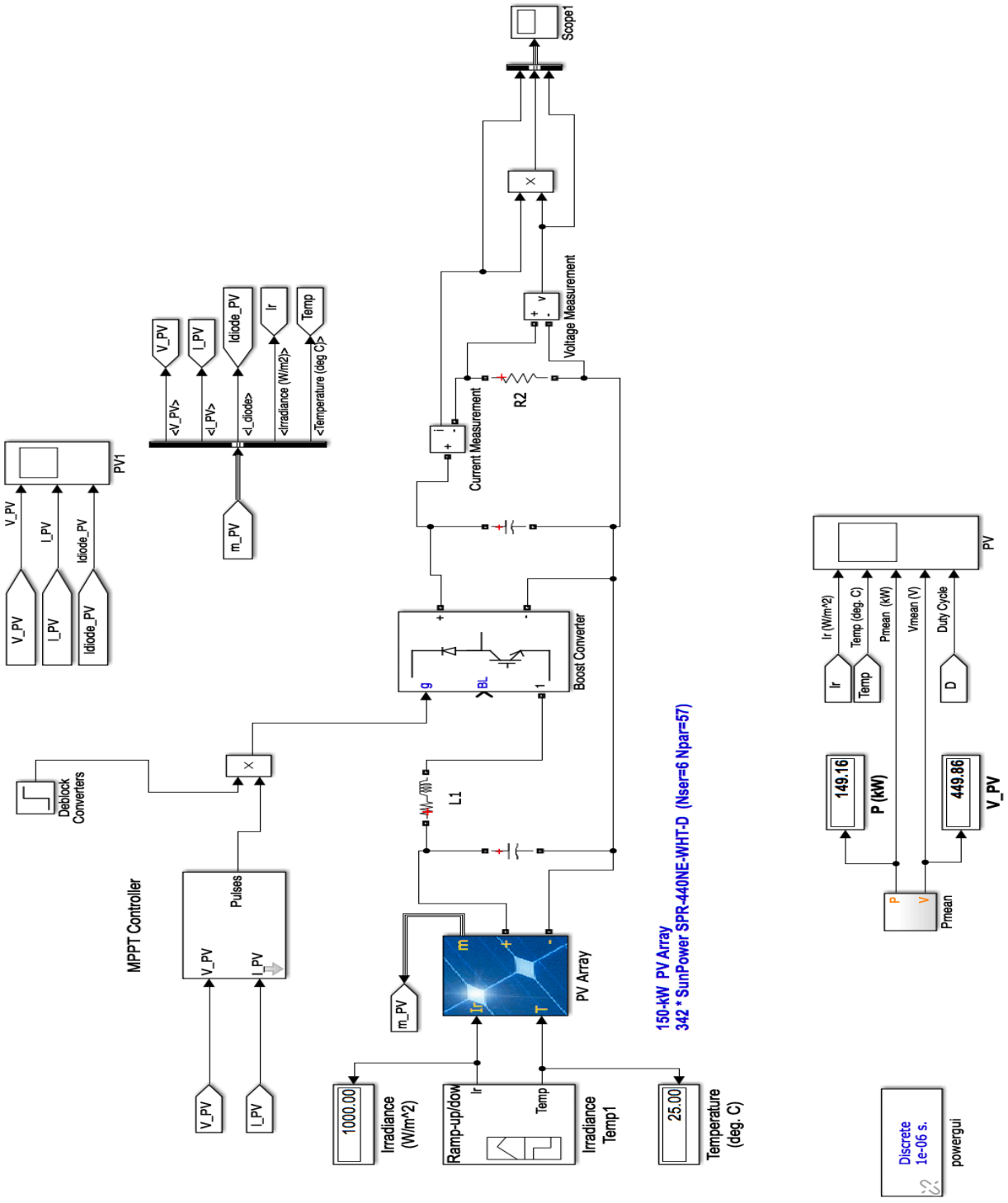

Figure 4.2 PV Solar System Design on MATLAB (Adapted from [36])

Figure 4.2 shows the architecture of the PV solar system designed for this thesis. This design is common for the three algorithms except for the MPPT controller block, where it differs for each of the algorithms in use. The three algorithms are: Perturb & Observe (P&O), Incremental Conductance with Integral regulator (INC), and finally Fuzzy Logic.

Figure 4.2 shows the components of the system, which are:

- PV Array (Model: Sun Power SPR- 440NE-WHT-D, 6S and 57P)
- MPPT Controller
- Boost Converter
- 2 Capacitors
- 2 Resistors
- 1 Inductor

The PV system design starts with a Ramp-up/ down module that controls and fluctuates the value of the temperature and the irradiance to simulate real life conditions. These values are being fed to the PV array block, which outputs a certain voltage and current depending on the specific values of the temperature and irradiance. The voltage and current values taken from the PV array are used as inputs to the MPPT controller while the output of the array is connected to a DC-DC Boost converter. The MPPT controller uses the input PV voltage and current value to continuously calculate the duty cycle, which is then fed to the boost converter. The boos converter controls the voltage level according to the duty cycle to keep tracking the Maximum Power Point at all times. Finally, the output of the boost converter is then connected to a resistive load, which acts as a demand side load for the stand-alone system.

4.2.1 Photovoltaic Module

There are various PV technology types including mono-crystalline silicon cells, multi-crystalline silicon cells, and amorphous silicon cells. The type chosen in this Thesis is the mono-crystalline silicon cell for their high efficiency. The solar panel that was chosen in this design is the Sun Power SPR- 440NE-WHT-D. Sun Power is a well-known manufacturer of solar panels and among the best in the market when it comes to a solar panel's performance.

Using MATLAB, the Sun Power SPR- 440NE-WHT-D module has the following specifications as shown in Table 4.1 [36]:

Table 4.1 PV Module Specifications

Number	Data	Value
1	Maximum Power	440.316 W
2	Cells per module	128
3	Open circuit voltage (Voc)	86.5 V
4	Short-circuit current (Isc)	6.5 A
5	Voltage at MPP (Vmp)	72.9 V
6	Current at MPP (Imp)	6.04 A
7	Temperature coefficient of Voc	-0.326 % / Deg.C
8	Temperature coefficient of Isc	0.019308 % / Deg.C

The modules in a PV system can be wired in series or in parallel depending on the output or power required. Wiring them in series increases the voltage while wiring them in parallel increases the current. The power, voltage, and current values are utilized to calculate the amount of modules to be connected in series in a string and

how many parallel strings are needed to reach the targeted output power. Therefore, using the values given in Table 4.1, the design has to have six modules connected in series in a string and 57 parallel strings to reach the required output power, which is 150 kW.

4.2.2 MPPT

4.2.2.1 Hill-climbing algorithm

The first type of MPPT is the hill-climbing algorithm. This Thesis uses two types of hill-climbing algorithms, which are P&O and INC+IR. Figure 4.3 shows the P&O function used in the MATLAB design. It has four inputs: (i) 'param', a parameter that has four variables, which are: initial, maximum, minimum, and increment values of the duty cycle; (ii) a constant 1 signal, to enable the function to operate; (iii) the PV voltage; and (iv) the PV current. This Simulink block utilizes a MATLAB code to calculate the duty cycle, PV output power, and PV output voltage. The code is shown in Appendix A.

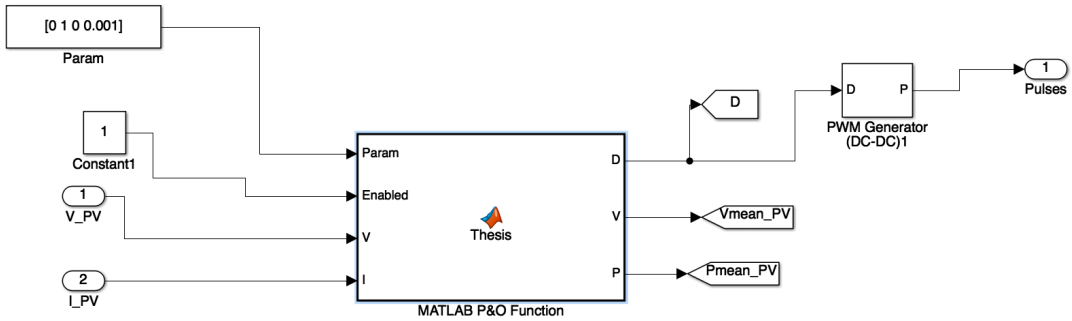

Figure 4.3 Simulink/MATLAB P&O Function

The second hill-climbing algorithm is the INC+IR. Figure 4.4 shows the Simulink block for this MPPT algorithm. Similar to the P&O, the INC+IR receives the PV voltage and current signals as inputs to produce the duty cycle. This block includes a

modified incremental conductance layout, which is the addition of the integral regulator in the end.

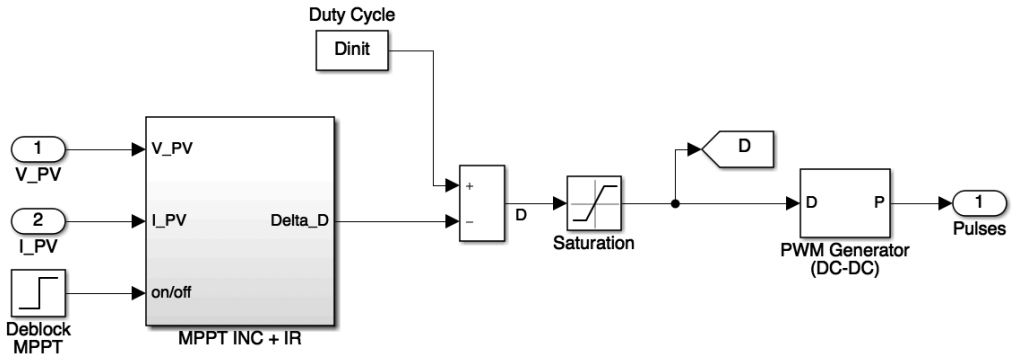

Figure 4.4 Simulink/MATLAB INC+IR MPPT Controller

4.2.2.2 Fuzzy Logic Controller

The second type of MPPT is the fuzzy logic controller. This controller is designed in a unique way as it utilizes linguistic rules and functions instead of mathematical models. Figure 4.5 shows the proposed MATLAB design of the fuzzy logic controller used in this Thesis. The fuzzy logic controller has two inputs, which are the error and the change in error as calculated using Equations 3.5 and 3.6 (refer to Section 3.3.5) and has one output, which is the duty cycle.

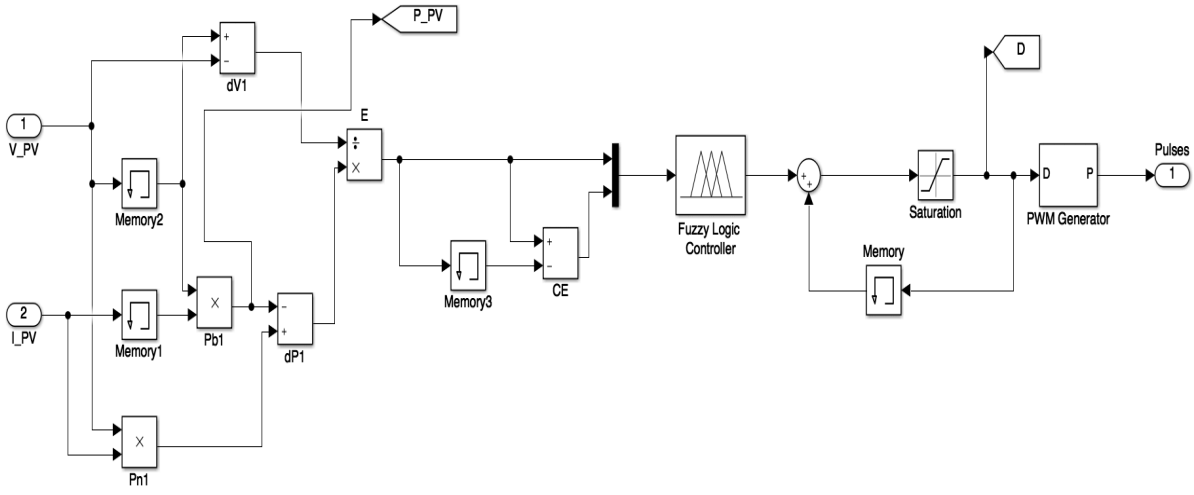

Figure 4.5 Simulink/MATLAB Fuzzy Logic MPPT Controller

Figures 4.6 to 4.8 show the fuzzy logic membership functions design window used for the error, change in error, and the duty cycle. All three of them have been designed using seven membership functions. These functions are labeled NB (Negative Big), NM (Negative Medium), NS (Negative Small), ZE (Zero), PS (Positive Small), PM (Positive Medium), and PB (Positive Big). The range chosen for the inputs is -6 to 6, while the range chosen for the output duty cycle is -0.1 to 0.1.

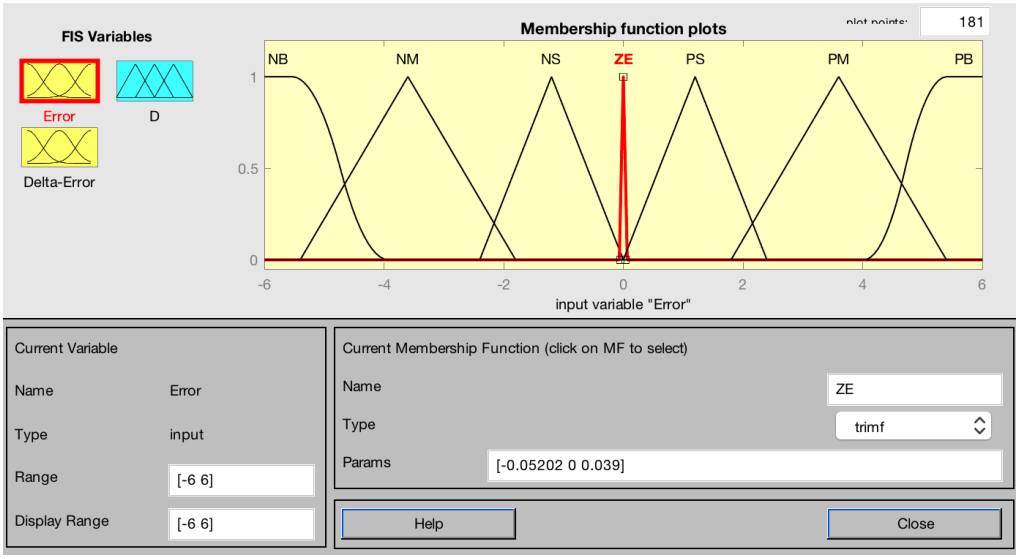

Figure 4.6 Input 1 Fuzzy Logic Membership Function

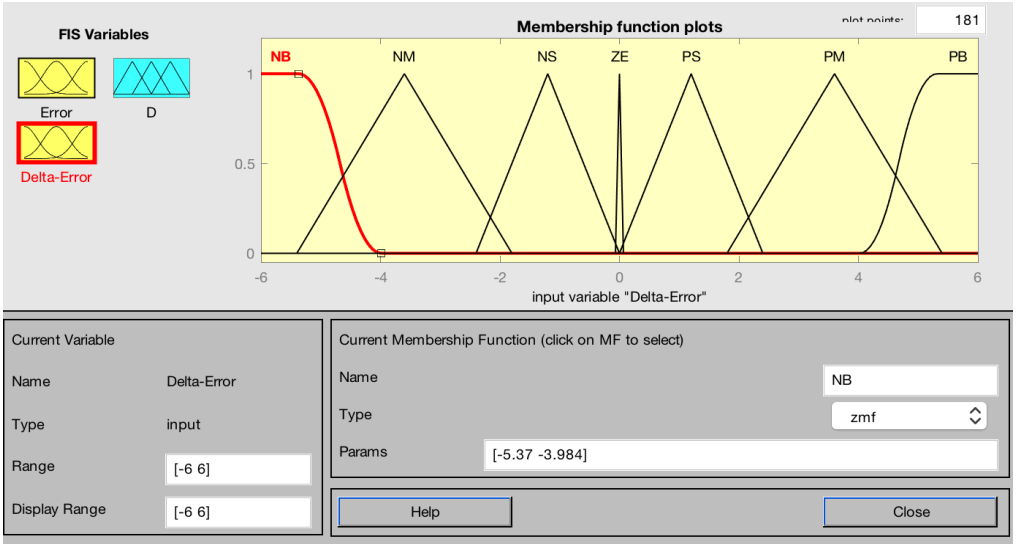

Figure 4.7 Input 2 Fuzzy Logic Membership Function

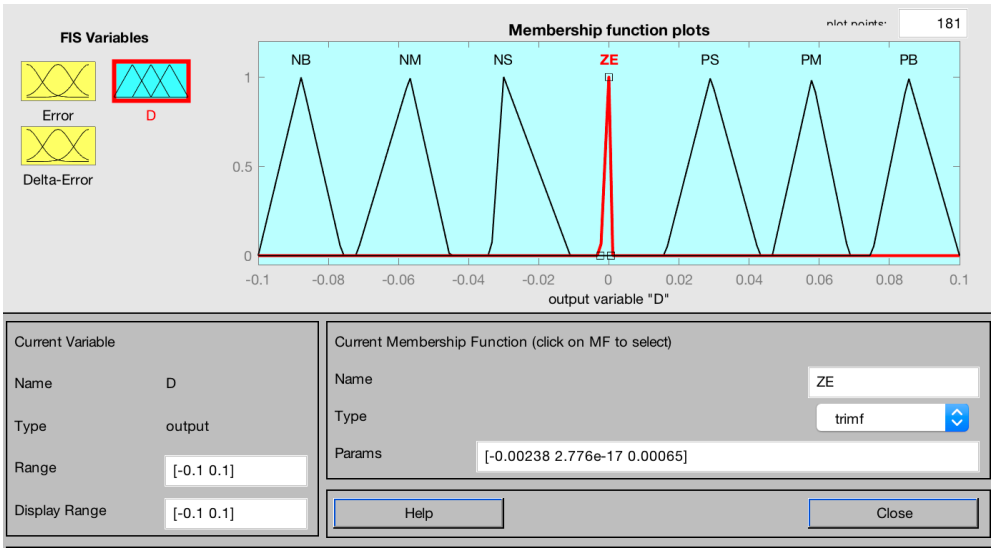

Figure 4.8 Output Fuzzy Logic Membership Function

Figure 4.9 shows the fuzzy rules design window. There are 49 proposed rules in this design, which are shown in Table 4.2. These rules can be modified based on each user's experience or by trial-and-error.

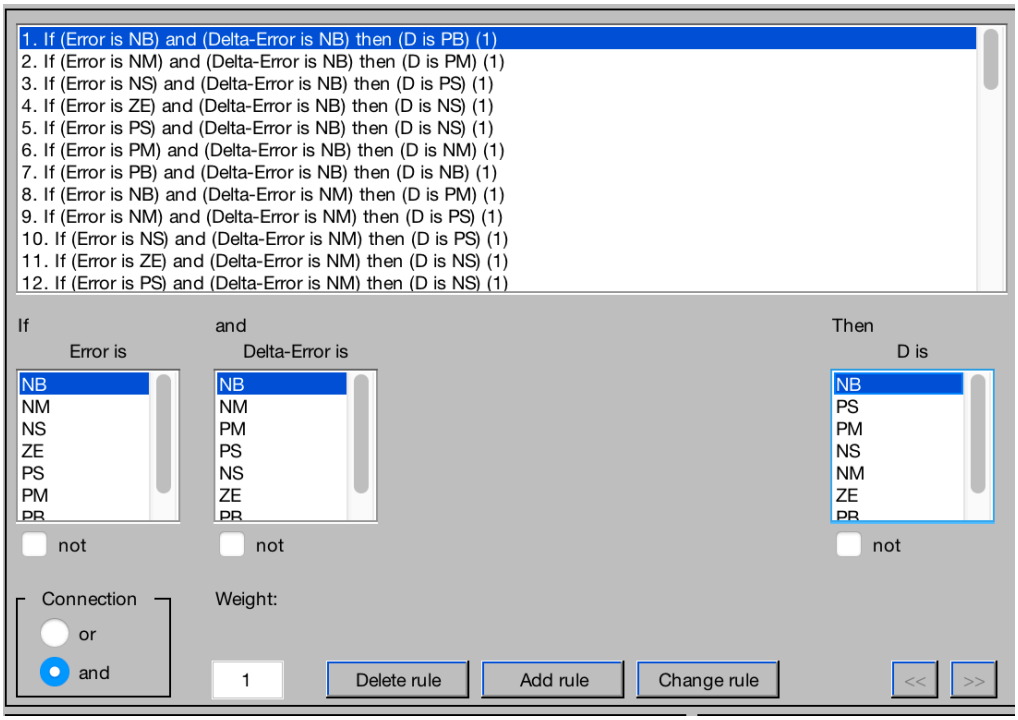

Figure 4.9 Fuzzy Rules Design Window

Table 4.2 Fuzzy Rules Table

Error / D-Error	NB	NM	NS	ZE	PS	PM	PB
NB	PB	PM	PS	NS	NS	NM	NB
NM	PM	PS	PS	NS	NS	NM	NB
NS	PS	PS	PS	PS	NS	NS	NM
ZE	NS	NS	NS	ZE	PS	PS	PS
PS	NS	NS	NS	ZE	PS	PS	PS
PM	NM	NS	NS	NS	PS	PS	PM
PB	NS	NM	NS	NS	PS	PS	PB

4.2.3 DC-DC Converter

The converter used in the design of this Thesis is a special type of DC-DC converter called boost converter. The boost converter is used to boost the output voltage and hence reduce the output current. This reduces the thermal losses due to the current. Figure 4.10 displays the basic components of a boost converter, which are: a diode, a switch, and at least one energy storage device. Normally, a Mosfet is used as a switch and the energy storage device is an inductor.

The operation of the boost converter is simple. There are two modes, one when the switch is closed, and the other when the switch is opened. Firstly, when the switch is closed, this means that the resistance in that wire is much lower than the load and thus the current will flow from the source and through that branch wire charging the inductor. The second state is the open state, which means that the diode is forward biased and all the current will be flowing through the diode and to the load including the energy that was stored in the inductor in the previous mode. This on-and-off

switching goes on continuously, and by adding the capacitor at the end, the output ripple due to switching can be filtered and can be approximated into DC output voltage [37].

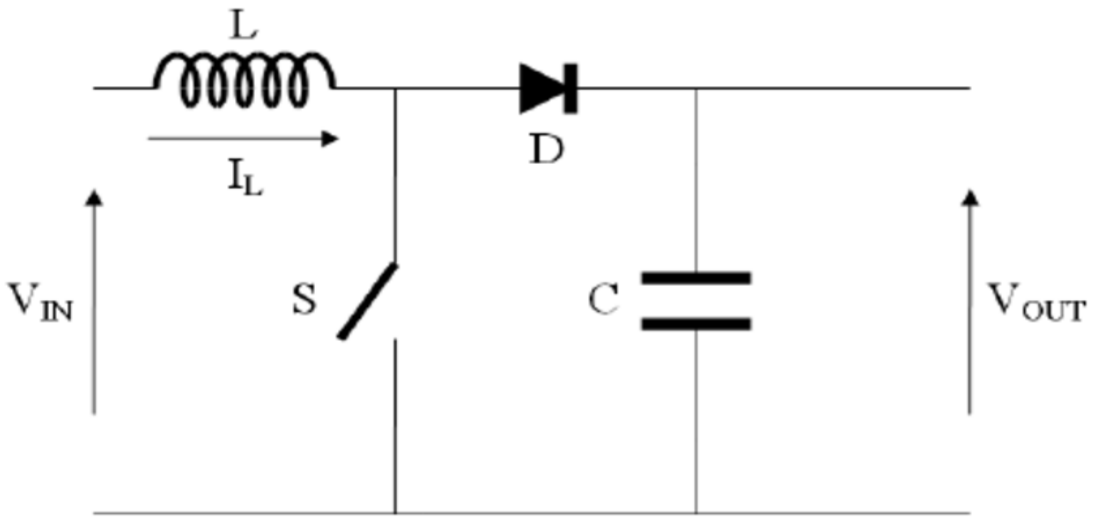

Figure 4.10 Boost Converter Circuit Diagram

Another major characteristic of the boost converter is that when it is used with an MPPT controller it is not only used to boost the voltage but also control it freely to reach the MPP. The MPPT controller uses different algorithms to produce the correct duty cycle value that is then fed to the boost converter to instruct it to manipulate the voltage to a certain direction to reach the MPP as fast and as accurate as possible.

The duty cycle value of the boost converter along with the capacitor and the inductor can be calculated using the Equations 4.1, 4.2, and 4.3 [38]:

$$\frac{Vout}{Vin} = \frac{1}{1-D} \tag{4.1}$$

Where:

Vout is the boost converter output voltage

Vin is the boost converter input voltage

D is the duty cycle value

Moreover, both the inductor and capacitor in the model can be designed using Equations 4.2 and 4.3:

$$L = \frac{Vin * Ton}{\Delta I_L} \tag{4.2}$$

Where:

L is the minimum value of the inductor

Vin is the boost converter input voltage

Ton is the turn on time of the transistor

ΔIL is the desired change in current ripple

$$C = \frac{I_{load} * Ton}{\Delta Vc} \tag{4.3}$$

Where:

C is the value of the capacitor

I_{load} is the current going through the load

Ton is the turn on time of the transistor

ΔVc is the desired change in voltage ripple

4.3 Effect of Temperature and Irradiance on the PV Output Power

There are several factors that affect the output of the PV system. Among these factors are: geographic location, meteorological conditions (such as amount of sunlight and snow), shading, dust and debris, irradiance, and temperature. Although all these factors have an effect on the output of the PV, the main factors that affect the operating conditions are the irradiance hitting the surface of the solar panel and the temperature of the panel itself.

This section presents the effect the temperature and irradiance have on the output parameters of the PV array. Figures 4.11 and 4.12 show the theoretical response of the chosen PV panel Sun Power SPR- 440NE-WHT-D with its specifications shown in Table 4.1 under varying temperature and irradiance.

The first factor discussed is the temperature, which may vary drastically in some parts of the world.

Figure 4.11 demonstrates the effect the module temperature has on the output power when the irradiance is kept constant at a value of 1000 W per square meter. The change in temperature of the module can occur due to numerous reasons. Some reasons include a change in atmospheric conditions such as the atmospheric temperature and degree of shading, or an artificial reason such as overheating as a result of improper maintenance of the panels. This change in the temperature usually affects the voltage output.

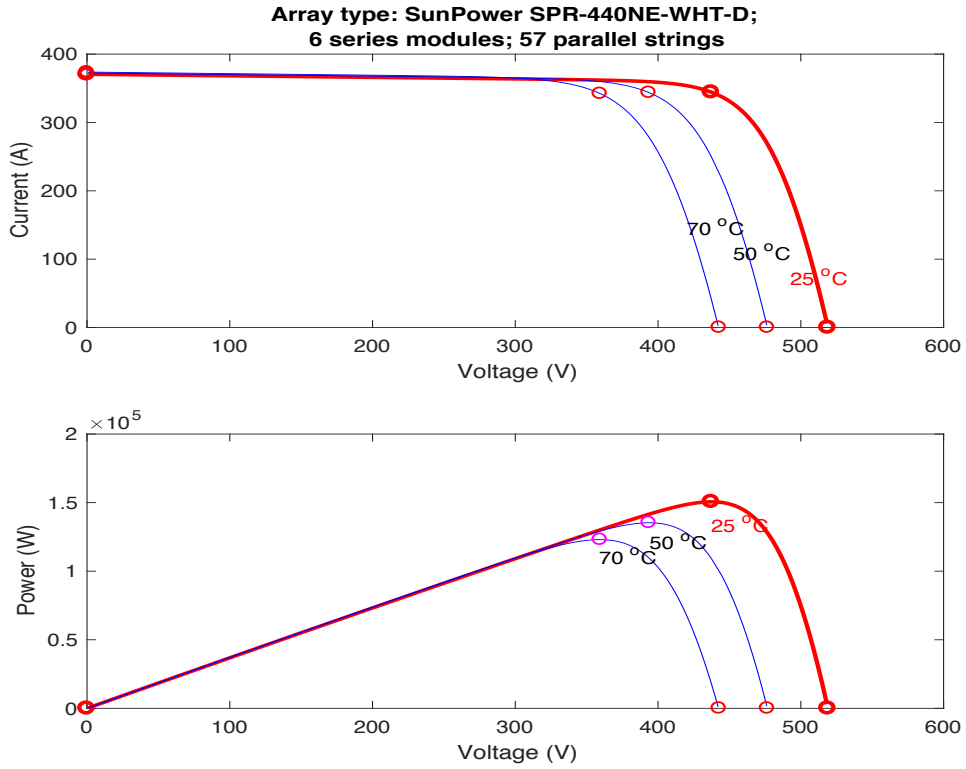

Figure 4.11 Effect of the Temperature on the Output Voltage, Current, and Power

As shown in Figure 4.11a, as the temperature increases, the output voltage drops significantly and this voltage drop is translated in Figure 4.11b as the effect on the output power. The output voltage and power were recorded using three different module temperatures, which are 25 ℃, 50 ℃, and 70 ℃. These temperature values were not randomly chosen but are actually the values in extreme conditions (25 ℃ and 70 ℃) as well as the average temperature value (50 ℃).

Normally, the temperature of the solar module is about 20 ℃ higher than the ambient temperature, so a temperature of 70 ℃ can be found in areas with an ambient temperature of 50 ℃ such as the Middle East during the summer. The other extreme is the panel temperature of 25 ℃, which would require an outside temperature of five degrees much like the Nordic countries. Finally, a temperature of about 40 ℃ to 50 ℃ is the common temperature of a panel at normal conditions. In Figure 4.11a, the voltage is highest at a value of higher than 500 Volts when the ambient temperature is 25 degrees, and drops down to roughly 480 and 450 Volts at temperatures of 50 and 70 ℃ respectively. The effect this current drop has on the power is shown in Figure 4.11b, where the power is again highest at temperature 25 ℃ with a value of 150 kW and reduces to 130 kW at 50 ℃ and drops even lower at 70 ℃.

The second factor discussed is the irradiance. Although it generally varies throughout the day and between different days, the total energy received from the sun each year is constant. As presented in Figure 4.12, the irradiance affects the cell's current value and they are directly proportional to each other.

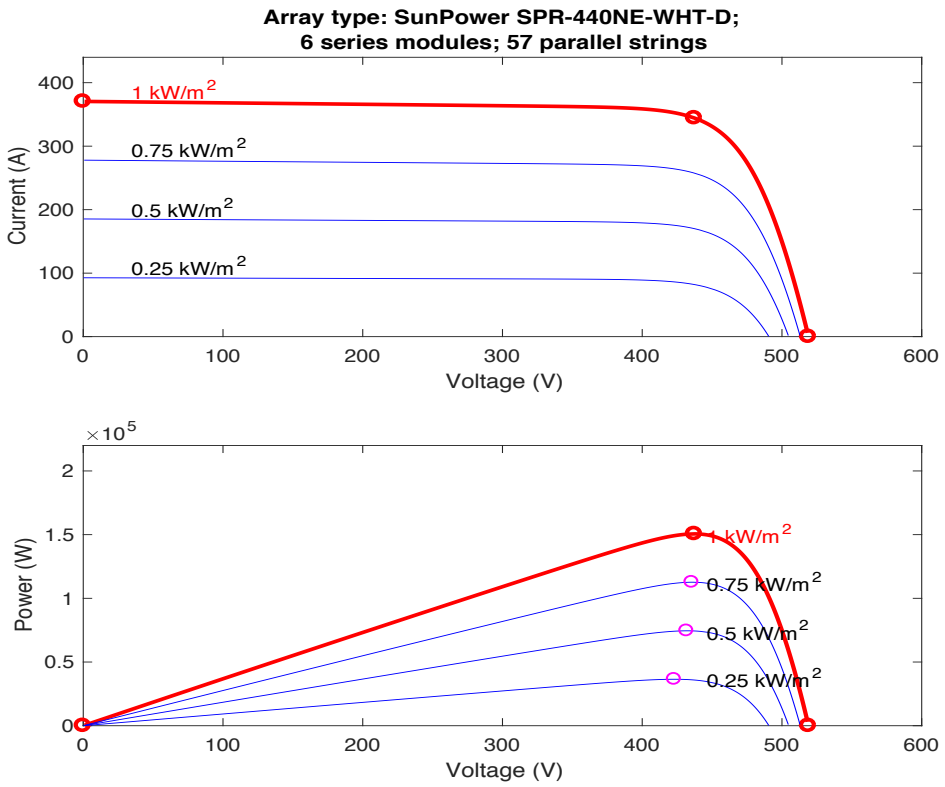

Figure 4.12 Effect of the Irradiance on the Output Voltage, Current, and Power

In Figure 4.12a, the effect the irradiance has on the current is shown where the current drops gradually from about 380 Amperes at 1000 W per square meter of irradiance to about 100 Amperes at 250 W per square meter of irradiance. The drop in irradiance results in a massive impact on the output power where it drops from 150 kW of power at 1000 W per square meter to 25 kW at an irradiance of 250 W per square meter.

Chapter 5 Discussion and Results

5.1 Introduction

The characteristics of the three chosen MPPT algorithms (P&O, INC., FLC) in the design model have been explained in Chapter Three. The outcome of using each algorithm in the solar system MPPT design is presented in this chapter.

There are three sections in this chapter that describe the results. These sections will highlight the performance of each individual controller under two separate scenarios. In the first scenario, the solar panel will be subjected to a constant solar irradiance of 1000 W per square meter and will have a constant internal temperature of 25 ℃ as shown in Figure 5.1. This allows for a simple and reliable comparison of the algorithms' performance in terms of accuracy and speed to get the desired power output, which is 150 kW.

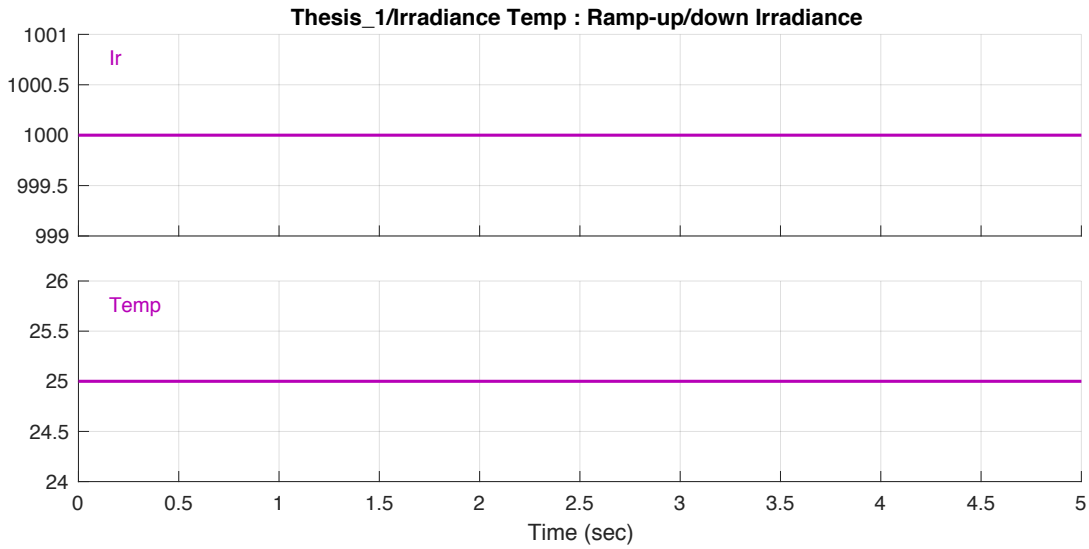

Figure 5.1 Constant Irradiance and Temperature Signals

Figure 5.2 illustrates the second scenario where the panel is subjected to variable irradiance and variable temperature to document the behavior of each algorithm when experiencing conditions similar to those in real life. The irradiance will vary from

1000 W per square meter to 250 W per square meter and the temperature will vary from 25 ℃ to 50 ℃. There is also a period of time where the temperature is constant and the irradiance is changing and vice versa and the reason behind that is to capture the effect of each of these variable on the output power separately.

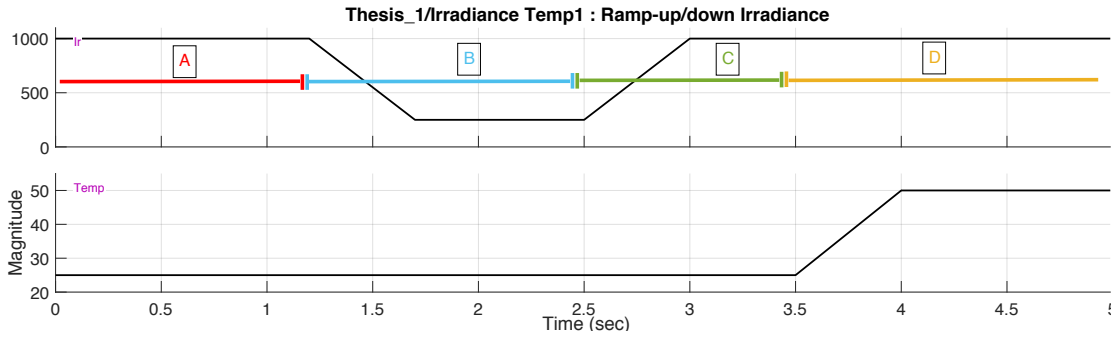

Figure 5.2 Varying Irradiance and Temperature Signals

These periods are shown in Figure 5.2. There are four periods labeled A, B, C, and D. Each of these periods represents a change occurring in either the irradiance or the temperature. Table 5.1 summarizes each period or stage:

Table 5.1 Comparison Between the Four Periods in the Design

Period	Color Code	Irradiance Value (W/m^2)	Temperature Value (℃)	Time range (Sec)
A	Red	1000	25	0 – 1.2
B	Blue	250 ≤ IV < 1000	25	1.2 – 2.5
C	Green	250 < IV ≤ 1000	25	2.5 – 3.5
D	Yellow	1000	50	3.5 – 5

As shown in Table 5.1, period A has a fixed value of irradiance and temperature at 1000 W per square meter and 25 ℃ respectively. In Period B the temperature remains unchanged, however, the irradiance drops from 1000 to 250 W per square meter and remains this way from the 1.7-second mark until 2.5 seconds. Period C commences

after the 2.5 second mark, increasing the voltage back to 1000 W per square meter. Finally, in period D, the first change in the temperature is witnesses from 25 ℃ to 50 ℃ while having an irradiance of 1000 W per square meter.

Sections 5.2, 5.3, and 5.4 contain two scenarios. In order to evaluate the results, each of these scenarios will contain the following three graphs:

- Change in Solar Irradiance and Ambient Temperature Versus Time
- System Output Power, Voltage, and Current Versus Time
- Duty Cycle, PV Voltage and Current, and System Output Voltage and Current Versus Time.

5.2 Perturb & Observe Algorithm Results

5.2.1 Scenario One: Constant Irradiance and Temperature

This section describes the simulation of the PV MPPT system under constant solar irradiance and module temperature where the irradiance is kept constant at 1000 W per square meter and the temperature at 25 ℃ (refer to Figure 5.1). When both variables are kept constant, the result will be as shown in Figure 5.3. The plot shows three lines using different color codes. As shown in the legend, blue is for the output power, red is for the output voltage, and finally, yellow is the output current.

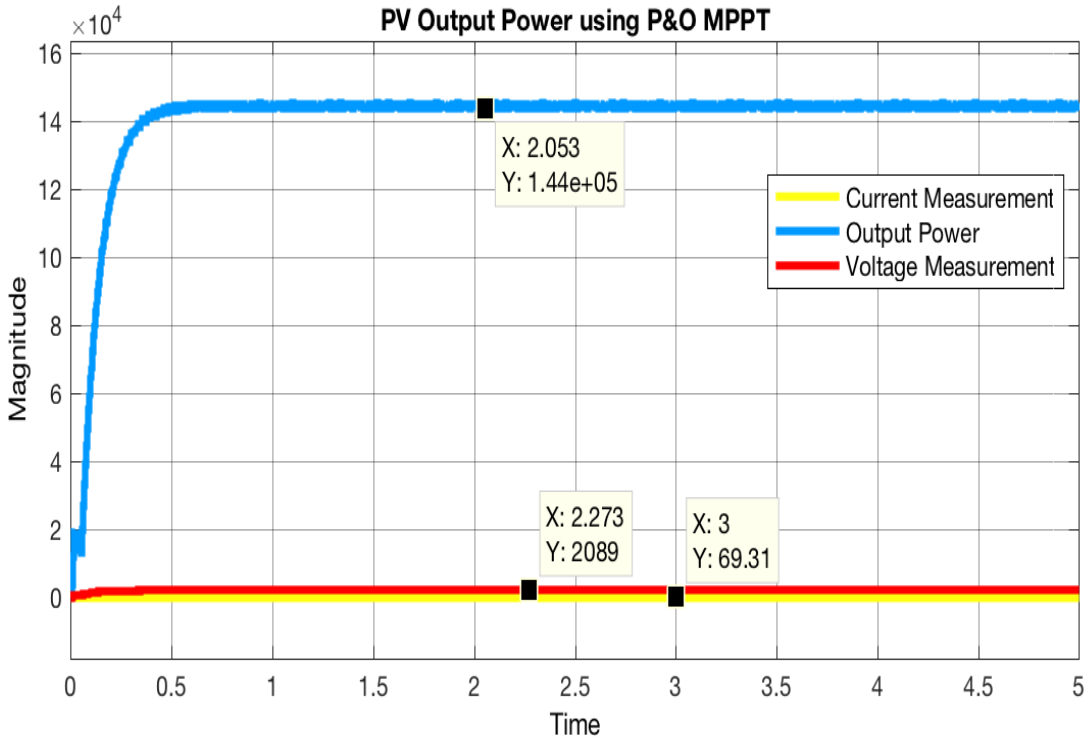

Figure 5.3 Output Power Under Constant Conditions Using P&O MPPT

Using the P&O algorithm yields a fast response as expected where the rise time is about 0.197 seconds or approximately 0.2 seconds and the settling time is about 0.26 seconds. The output power starts from zero and reaches a maximum value of 145,500 W at time 4.15 seconds. However, as shown in Figure 5.3, the P&O method results in continuous oscillations around the Maximum Power Point. This is clearly presented in Figure 5.4 where a segment of the output power was magnified to illustrate these oscillations. The chosen segment is an interval of about 0.3 seconds where it starts at time around 3.4 seconds and ends at about 3.7 seconds. During this interval, the power fluctuates between the values of 144,000 W and 145,400 W with a mean value of about 144,800 W.

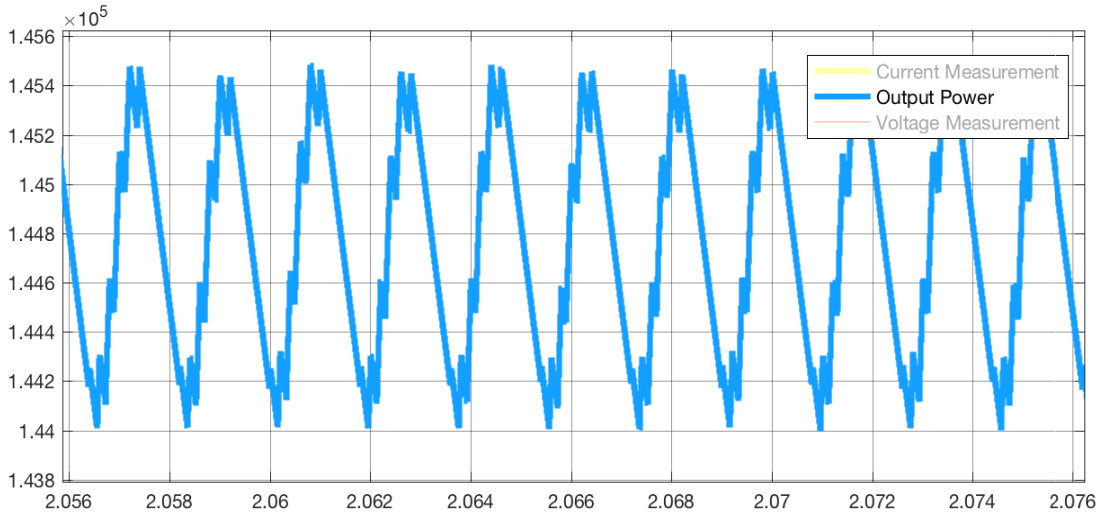

Figure 5.4 Output Power Oscillations when Using P&O

The mean for the curve was calculated to be about 144,600 W. The target output power is 150,000 W and hence the system's efficiency when using P&O method at constant irradiance and temperature is 96.4%. Figure 5.5 is divided into 5 plots, which are; the duty cycle (DC), the PV output voltage, PV output current, system output voltage, and current on the load side. The first graph shows the duty cycle oscillations. The DC starts oscillating between 0 and 1 in the beginning, but as the output voltage and current reach their respective steady state value, the DC is confined between 0.4 and 1. The second and third graphs represent the voltage and current produced by the PV panel. The voltage oscillates heavily around the value of 400 Volts and similarly the current oscillates around 300 Amperes. The last two graphs are the output or the load side voltage and the current, which are the voltage and current output from the PV panel after passing through the boost converter. As previously mentioned in Chapter 4, the function of the boost converter is to increase the voltage, decrease the current to reduce the current losses, and reduce both the voltage and current ripples caused by the constant switching. This matches with the results where the voltage was amplified to 2000 Volts, the current reduced to about 60 Amperes, and both curves were smooth and non-oscillating.

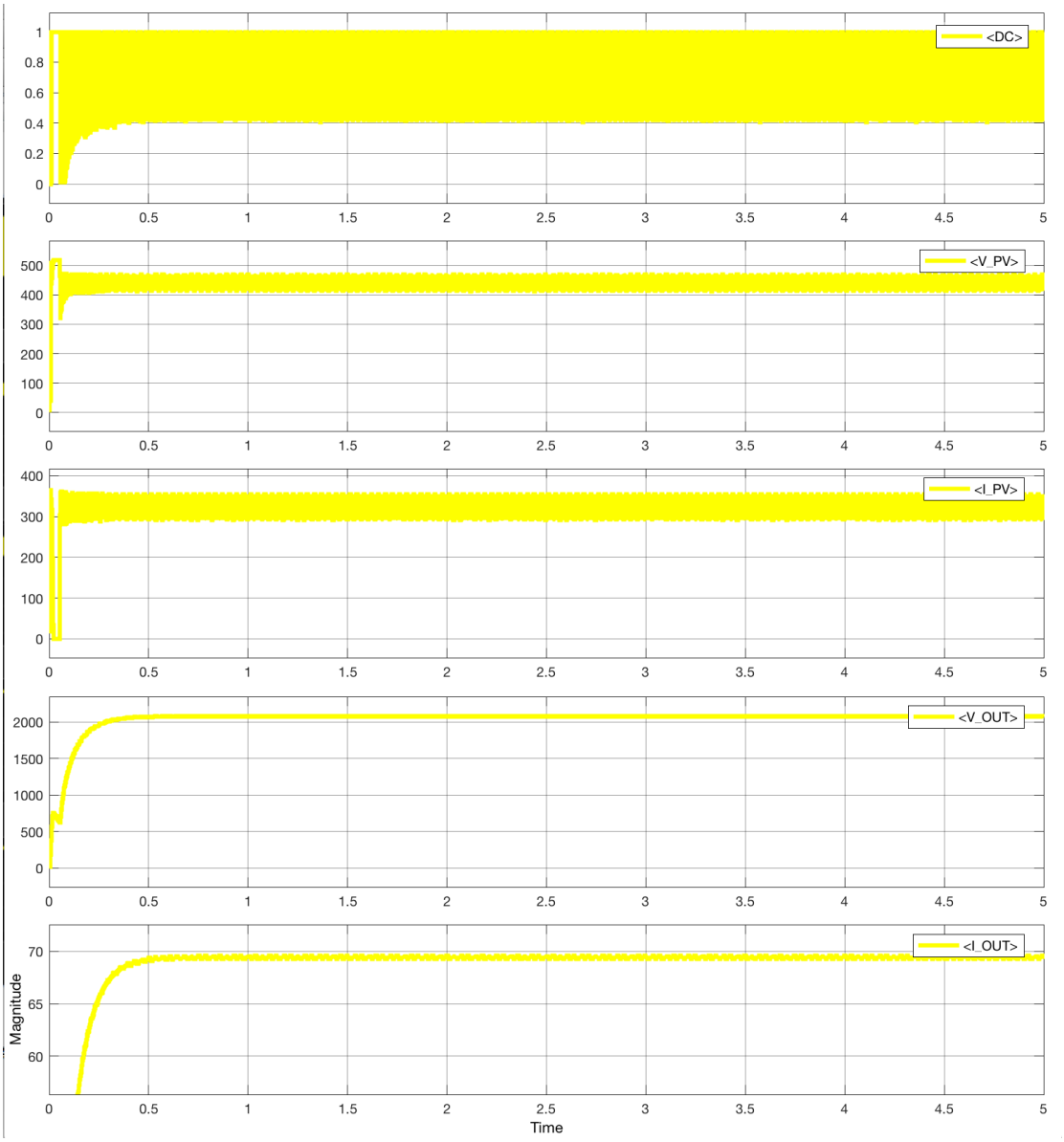

Figure 5.5 P&O DC, Voltage and Current Diagrams Under Constant Conditions

5.2.2 Scenario Two: Varying Irradiance and Temperature

As explained in section 5.1, there are 4 periods in the second scenario. Each period has either the irradiance or temperature varied from the previous period as shown in Figure 5.6. There are two conclusions that can be drawn from this scenario; the first is regarding the effect of the irradiance and temperature individually on the output

power, and the second is about the efficiency of the MPPT algorithm used. In this case, it is the P&O used in generating power under varying conditions.

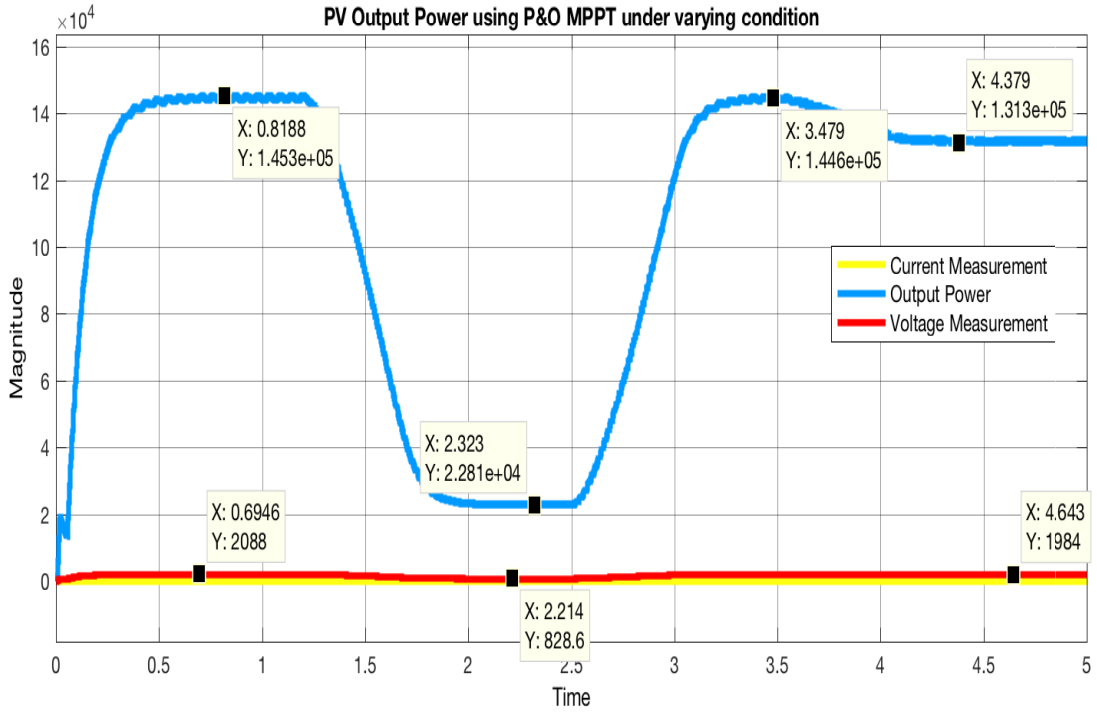

Figure 5.6 Output Power Under Varying Conditions Using P&O MPPT

In Figure 5.6, period A has an irradiance of 1000 W per square meter and module temperature of 25 ℃ and has the output power curve increasing from zero to 144,700 W of power. It drops down to about 22,990 W in period B when the irradiance is dropped to 250 W per square meter and the temperature is kept constant. In part C, the irradiance is increased again to 1000 W per square meter and thus the power output is close to that in part A which is 144,400 W. Part C is done in preparation for part D, where the irradiance is kept constant at 1000 W per square meter and the temperature is increased from 25 to 50 ℃. This results in a power output drop from 144,400 W to 131,600 W.

As expected, the irradiance has a substantial effect on the output power where a 75% decrease in the irradiance causes about an 84% drop in the output power as shown in

part B. Moreover, when the module temperature doubles from 25 to 50 ℃, the power output reduces by about 9%.

Even though the drop in power output in the two cases where the irradiance decreases or where the module temperature increases was anticipated, it is how efficient the actual output of the P&O is compared to the theoretical values when the variations occurred.

Table 5.2 shows the actual output power measured at each of the periods along with the theoretical output powers that are calculated using the MATLAB solar panel block. This block calculates the theoretical output power at given irradiances and module temperatures. The efficiency of the PV system using the P&O method can be calculated using Equation 5.1:

$$EFF = \frac{AP}{THP} \times 100\% \tag{5.1}$$

Where:

EFF is the Efficiency percentage
THP is the theoretical power
AP is the actual power

Table 5.2 P&O Efficiency Percentages of each Period

Period	Irradiance Value (W/m^2)	Temperature Value (℃)	Actual Output Power (W)	Theoretical Output Power (W)	Efficiency Percentage %
A	1000	25	144,700	150,600	96.08
B	250	25	22,900	36,460	62.81
C	1000	25	144,400	150,600	95.88
D	1000	50	131,600	135,300	97.27

Using Equation 5.1 results in an efficiency of about 96% in period A, 62.8% in period B, 95.88% in period C, and 97.27% in period D. This shows that while the irradiance is at a high level, the efficiency of the MPPT is quite high at approximately 96% even at times of increased temperature. On the other hand, when the irradiance value drops so does the efficiency percentage where the reported percentage is 62.8% at an irradiance level of 250 W per square meter.

Figure 5.7 P&O DC, Voltage and Current Diagrams Under Varying Conditions

The last part of this scenario (and section) is Figure 5.7. This figure shows the duty cycle values, PV output voltage and current, and the system output voltage and current. Similar to the first scenario, the PV output voltage and current oscillate heavily until they pass through the boost converter, which allows for a boost in voltage, a drop in current, and removing the oscillations from both curves. Moreover, an observation in the PV voltage and current curves is that while a decrease in irradiance affects both these variables as shown in period B, the PV current is affected more. The current drops from an average of 320 Amperes to an average of 80 Amperes, while the voltage only drops from an average of 450 Volts to about 350 Volts. On the other hand, an increase in the temperature affects the PV voltage where it drops from 450 Volts to about 400 Volts; however, the temperature spike from 25 ℃ to 50 ℃ has an insignificant effect on the current that does not manifest on the curve. Finally, the voltage and current of the output system seem to react in a similar manner where they are both affected similarly during the drop in irradiance and rise in temperature. The output voltage starts at 2100 Volts in period A, drops to about 850 Volts in period B, goes back up to 2100 Volts in period C and finally reduces a bit more to 2000 Volts in period D. Likewise, the output current starts at 70 Amperes, drops to 28 Amperes, back to 68 Amperes, and finally reduces to about 66 Amperes.

5.3 Incremental Conductance +Integral Regulator

This section is dedicated towards presenting the results of using the incremental conductance algorithm with an integral regulator as a Maximum Power Point Tracker.

5.3.1 Scenario One: Constant Irradiance and Temperature

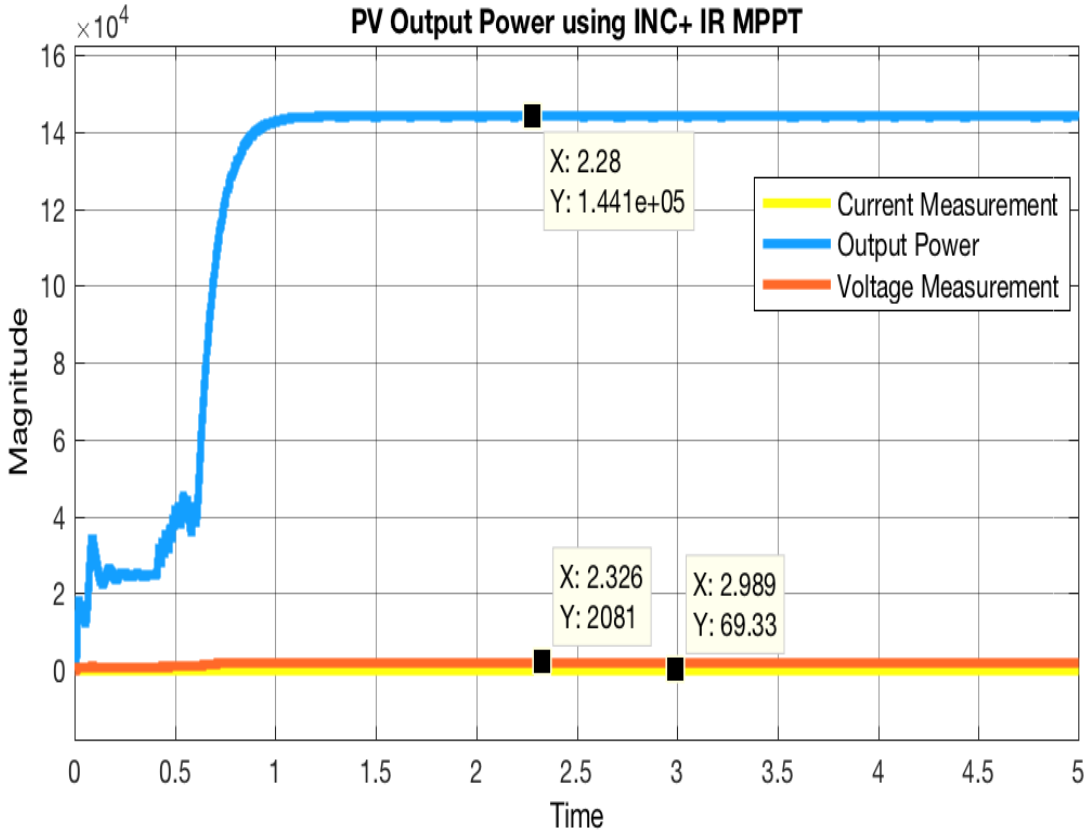

Figure 5.8 Output Power Under Constant Conditions Using INC MPPT

The INC algorithm in Figure 5.8 results in a rise time of the output power of about 0.216 seconds, which is similar to the rise time when using the P&O algorithm. However, the settling time, which is about 0.8 seconds, is rather high and this delay is caused by the addition of the integral regulator to the INC algorithm. The integral regulator was added to reduce the steady state error of the output power where the output power is 144,100 W and the targeted output power is 150,000 W. This output power means that the INC algorithm has an output efficiency of about 96.06%

Moreover, as shown in Figure 5.8, there are no visible oscillations unlike the P&O algorithm where the output keeps on perturbing constantly. The INC algorithm does oscillate, however it does so with small amplitude that it is considered negligible.

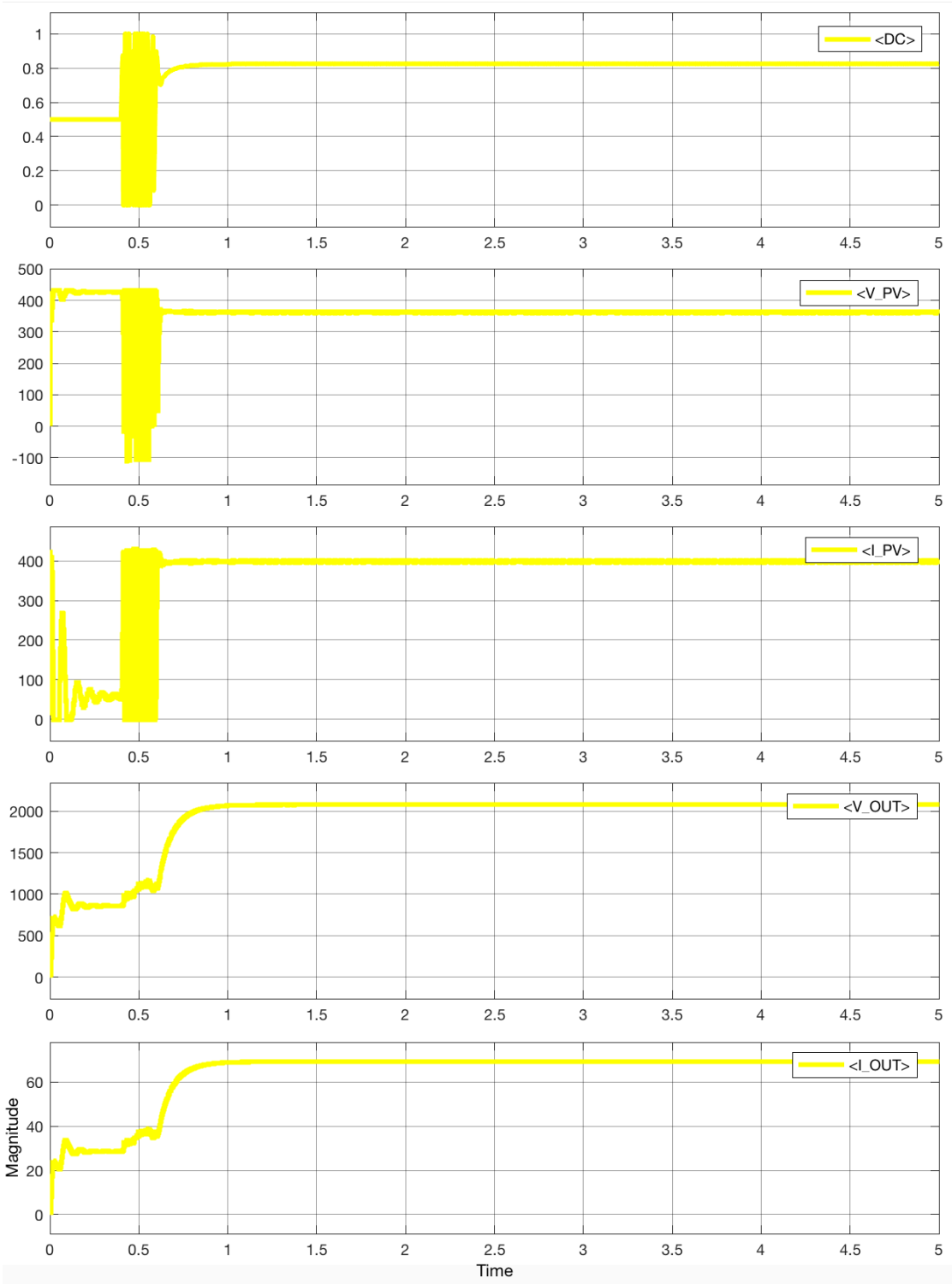

Figure 5.9 INC DC, Voltage, and Current Diagrams Under Constant Conditions

Figure 5.9 shows the duty cycle values, PV output voltage and current, and the system output voltage and current when using INC under constant conditions. The first noticeable feature in the graphs is the lack of oscillations, unlike the P&O algorithm.

The PV current and voltage graphs presented in Figure 5.9 only oscillate at the very beginning and even these oscillations are nearly straightened out by the boost converter in the last two curves of the system's output voltage and current. All the curves reach their steady state value at around 0.8 seconds where the Duty Cycle's value is about 0.8246, the PV voltage is 365.7 Volts, PV current is 396.6 Amperes, and the system's output voltage and current are at 2081 Volts and 69.36 Amperes respectively.

5.3.2 Scenario Two: Varying Irradiance and Temperature

This section displays the output results when using INC MPPT under varying conditions.

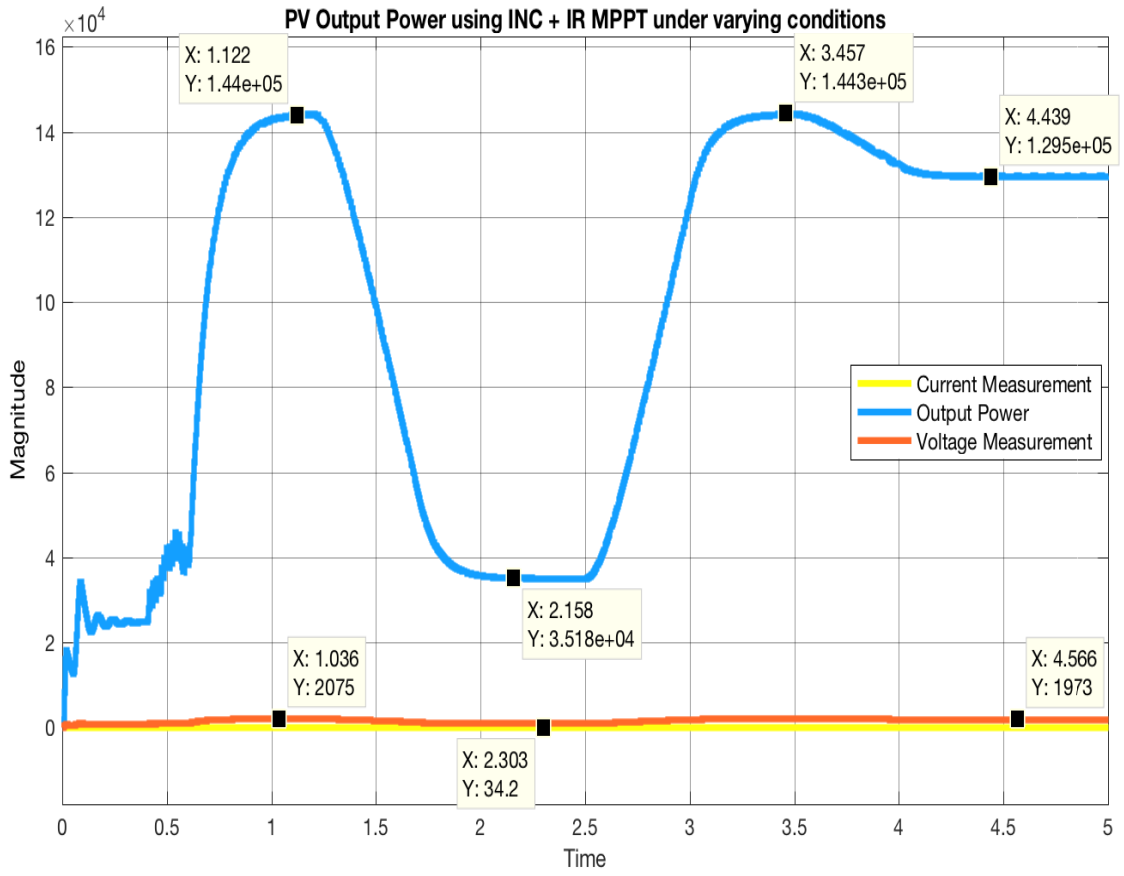

Figure 5.10 Output Power Under Varying Conditions Using INC MPPT

In Figure 5.10, period A is where the irradiance is 1000 W per square meter and the module temperature is 25 ℃ with the output power curve increasing from zero to 144,000 W of power. The output power then drops down to about 35,180 W in period B when the irradiance drops to 250 W per square meter and the temperature is kept constant. In part C, the irradiance increases again to 1000 W per square meter and thus the power output is close to that in part A which is 144,100 W. Part C is done in preparation for part D, where the irradiance is kept constant at 1000 W per square meter and the temperature is increased from 25 to 50 ℃. This results in a power output drop from 144,400 W to 129,500 W.

Similar to the P&O controller, in the INC+IR, the drop in the irradiance caused the most inclination in output power where the change from 1000 W per square meter to 250 W per square caused a 75.6% drop in the output power. On the other hand, the increase in temperature from 25 ℃ to 50 ℃ caused a percentage drop in power by about 10%.

Table 5.3 INC Efficiency Percentages of each Period

Period	Irradiance Value (W/m^2)	Temperature Value (℃)	Actual Output Power (W)	Theoretical Output Power (W)	Efficiency Percentage %
A	1000	25	144,000	150,600	95.61
B	250	25	35,180	36,460	96.49
C	1000	25	144,100	150,600	95.68
D	1000	50	129,500	135,300	95.71

Table 5.3 demonstrates the efficiency levels that were calculated using Equation 5.1, which are: 95.6% in period A, 96.5% in period B, 95.7% in period C and 95.7% in

period D. Even though the efficiency levels for period A, C, and D are almost equal to the P&O levels, there is a massive difference in period B where the INC algorithm coupled with the integral regulator, is able to stay consistent in terms of efficiency levels even during times with low irradiance. INC + IR is able to keep an efficiency above the 95% rate at all times especially during varying weather conditions unlike P&O, which scored a modest 62.8% when the irradiance level dropped to 200 W per square meter.

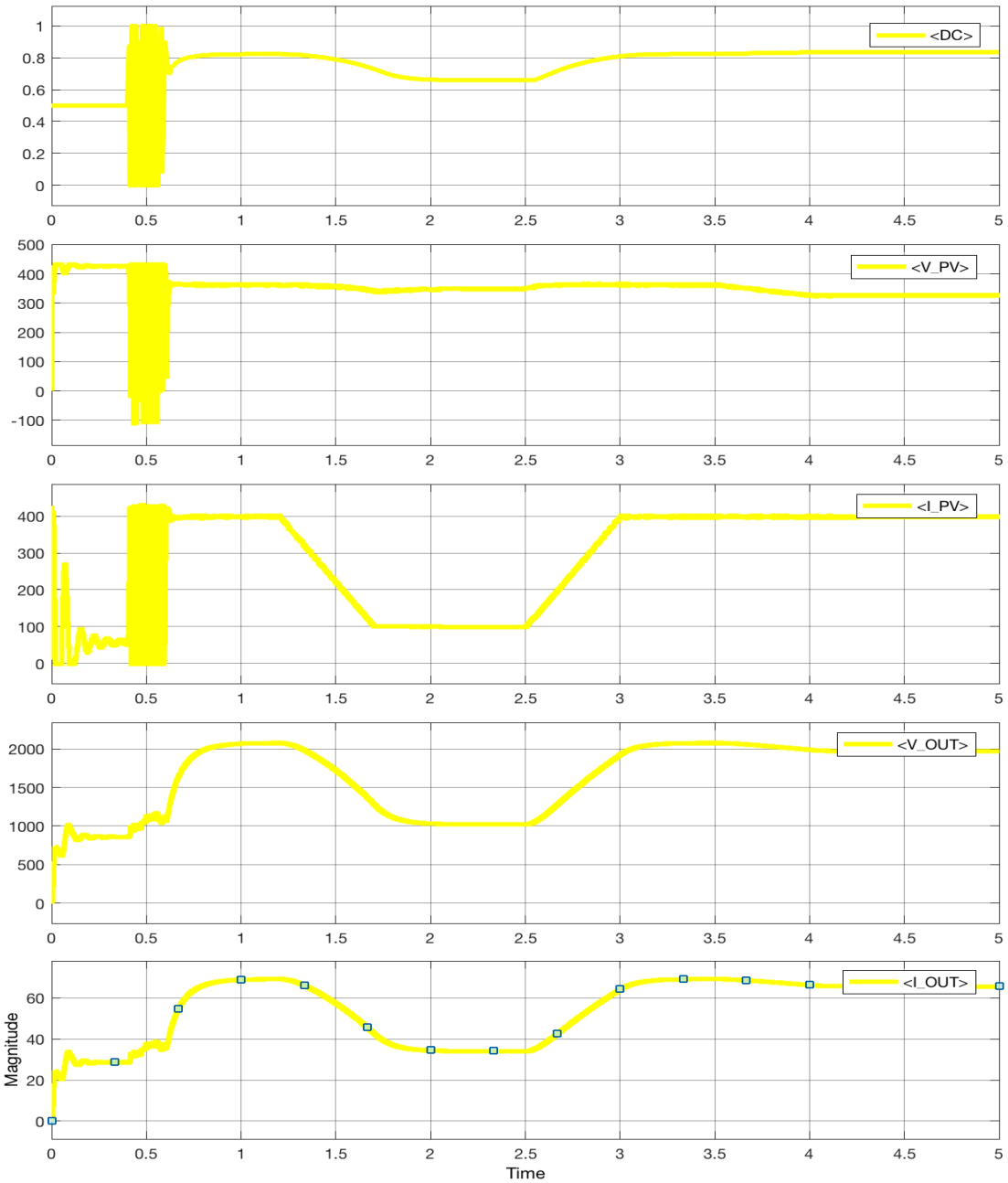

Figure 5.11 INC DC, Voltage, and Current Diagrams Under Varying Conditions

Figure 5.11 shows the duty cycle values, PV output voltage and current, and finally the system output voltage and current. Regarding the PV's voltage and current behavior, the current is highly affected by the drop in the irradiance from 399 Amperes to about 100 Amperes and does not show a significant effect during the increase in temperature. However, the PV voltage does not seem to be affected much by either change but is affected more by the temperature where it drops from 363 Volts in period A to 349 Volts in period B and 326 Volts in period D. The two final curves in Figure 5.11 are of the load side voltage and current, which react in the same manner they start at with values of 2075 Volts and 69 Amperes respectively in period A, dropping to 1028 Volts and 34.3 Amperes in period B, increasing back to 2080 Volts and 69 Amperes in period C, and finally slightly dropping to 1972 Volts and 65.7 Amperes in period D.

5.4 Fuzzy Logic Controller

This section is dedicated to presenting the results of using Fuzzy Logic Controller as a Maximum Power Point Tracker.

5.4.1 Scenario One: Constant Irradiance and Temperature

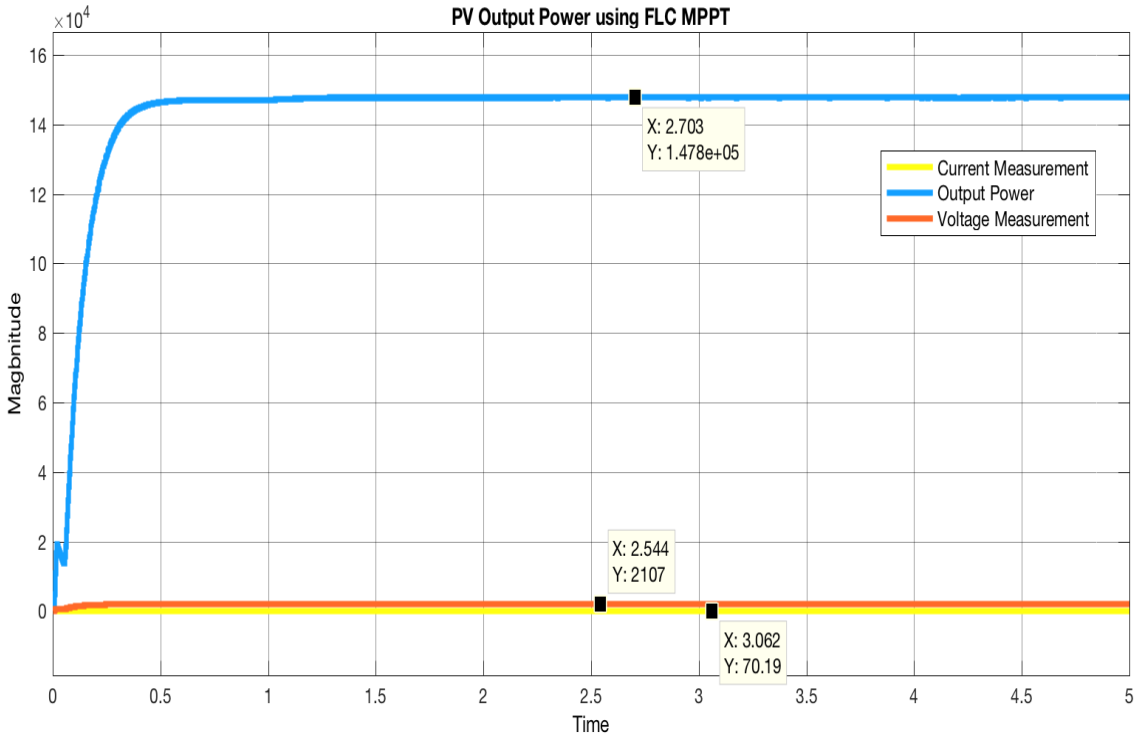

Figure 5.12 Output Power Under Constant Conditions Using FLC MPPT

The step response of the output power using fuzzy logic controller in Figure 5.12 results in a rise time of the output power of about 0.198 seconds and settling time of about 0.26 seconds. This is similar to the P&O algorithm but faster than the INC algorithm. Moreover, the output power reaches a maximum value of about 148,100 W at time 4.675 seconds. However, the mean value of the output power is 148,000 W and when compared to the targeted output power, which is 150,000 W, results in an output efficiency of about 98.66% for the FLC.

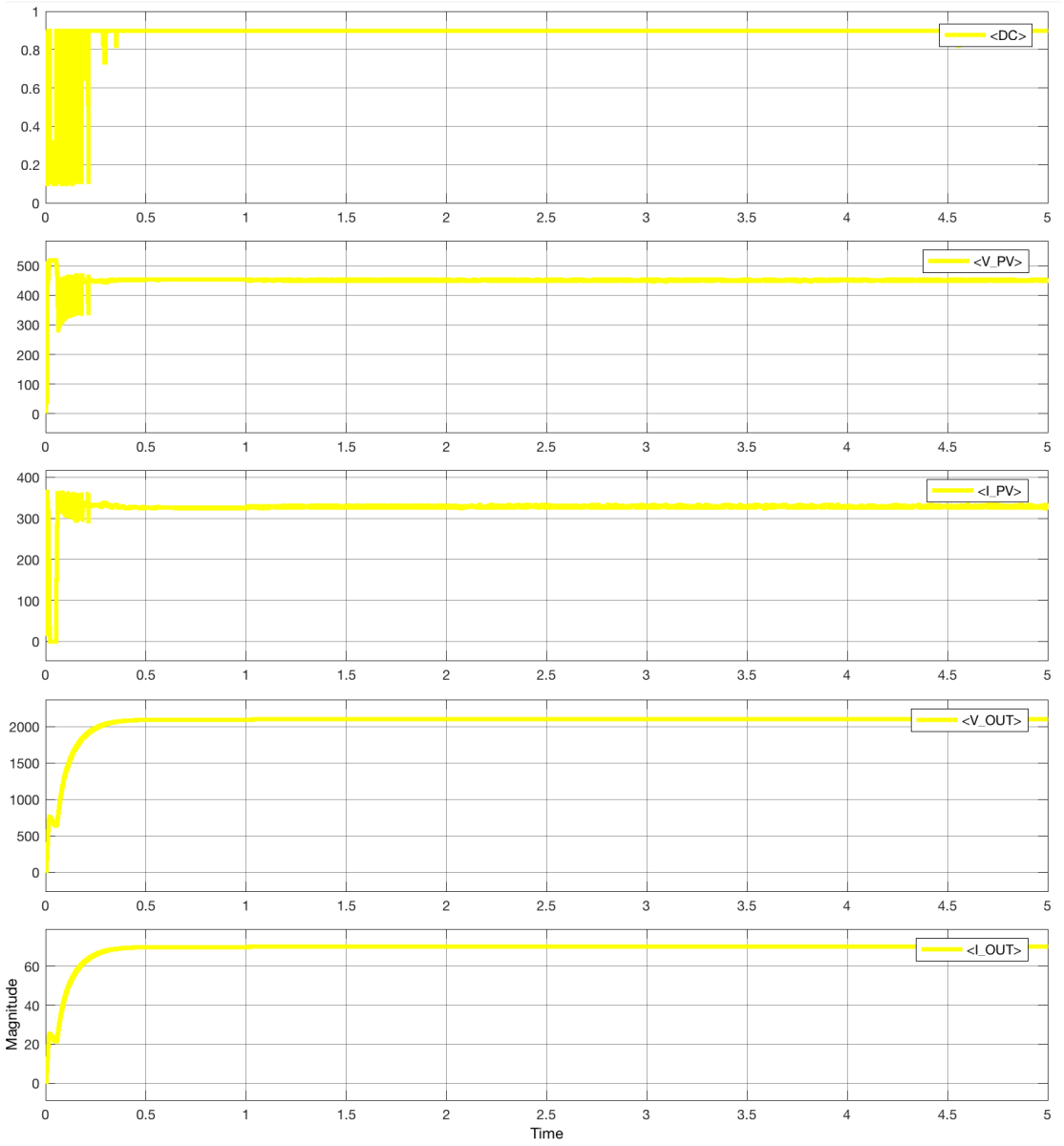

Figure 5.13 FLC DC, Voltage, and Current Diagrams Under Constant Conditions

Figure 5.13 is divided into 5 plots under constant weather conditions, which are: the duty cycle (DC), the PV output voltage, PV output current, system output voltage, and current on the load side. The first three graphs oscillate at the very beginning until they reach their steady state value at time of about 0.3 seconds. The steady state values are: 0.9 for the DC, 452 Volts for the PV voltage, 326.2 Amperes for the PV current, 2106 Volts for the output system voltage, and 70.2 Amperes for the output system current.

5.4.2 Scenario Two: Varying Irradiance and Temperature

This section displays the output results when using the FLC MPPT under varying conditions.

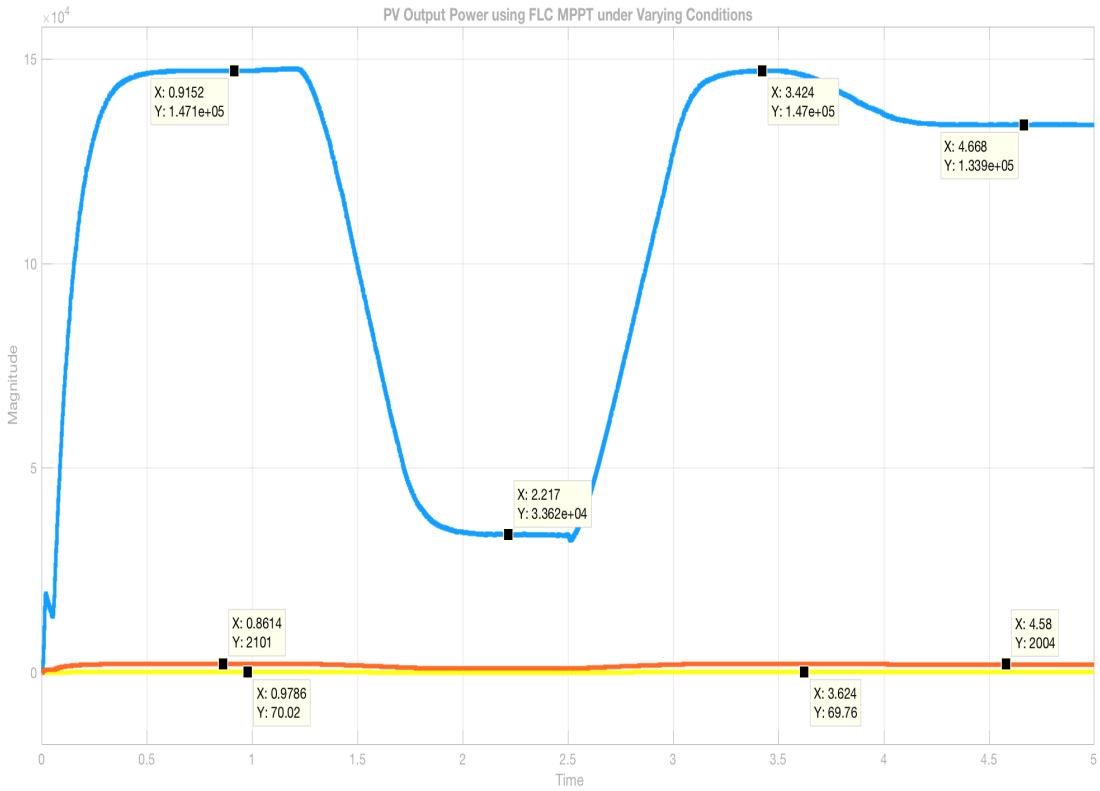

Figure 5.14 Output Power Under Varying Conditions Using FLC MPPT

In Figure 5.14, period A is where the irradiance is 1000 W per square meter and the module temperature is 25 ℃. The output power curve increases here from zero to 147,600 W of power. It then drops down to about 33,770 W in period B when the irradiance drops to 250 W per square meter and the temperature is kept constant. In part C, the irradiance increases again to 1000 W per square meter and thus the power output is close to that in part A, which is 147,200 W. Part C is done in preparation for part D, where the irradiance is kept constant at 1000 W per square meter and the temperature increases from 25 to 50 ℃. This results in a power output drop from 147,200 W to 133,900 W.

Similar to sections 5.2 and 5.3, the drop in the irradiance causes the most deterioration in output power where the change from 1000 W per square meter to 250 W per square caused a 77.2% drop in the output power. On the other hand, the increase in temperature from 25 ℃ to 50 ℃ causes a percentage drop in power by about 9%.

Table 5.4 demonstrates the efficiency levels calculated using Equation 5.1, which are: 98.0% in period A, 92.43% in period B, 97.74% in period C, and 98.97% in period D. FLC achieved staggering efficiency percentages across all four periods. The efficiency levels are higher than both P&O algorithm and INC + IR except for period B where FLC is trailing behind the Incremental Conductance algorithm, but not by a large amount but is still quite efficient (92%)

Table 5.4 FLC Efficiency Percentages of each Period

Period	Irradiance Value (W/m^2)	Temperature Value (℃)	Actual Output Power (W)	Theoretical Output Power (W)	Efficiency Percentage %
A	1000	25	147,600	150,600	98.00
B	250	25	33,700	36,460	92.43
C	1000	25	147,200	150,600	97.74
D	1000	50	133,900	135,300	98.97

Figure 5.15 shows the Duty cycle values, PV output voltage and current, and the system output voltage and current. Regarding the PV's voltage and current response, the current is highly affected by the drop in the irradiance from 326 Amperes to about a mean value of 75 Amperes and no change is observed during the increase in temperature. However, the PV voltage does not seem to be affected much by either change but is affected more by the temperature where it drops from 453 Volts in period A to 451 Volts in period B and 401 Volts in period D. The two final curves are

of the load side voltage and current which react in the same manner they start at with values of 2101 Volts and 70.04 Amperes respectively in period A, dropping to 1006 Volts and 33.5 Amperes in period B, increasing back up to 2101 Volts and 70.03 Amperes in period C, and finally slightly dropping to 2005 Volts and 66.8 Amperes in period D.

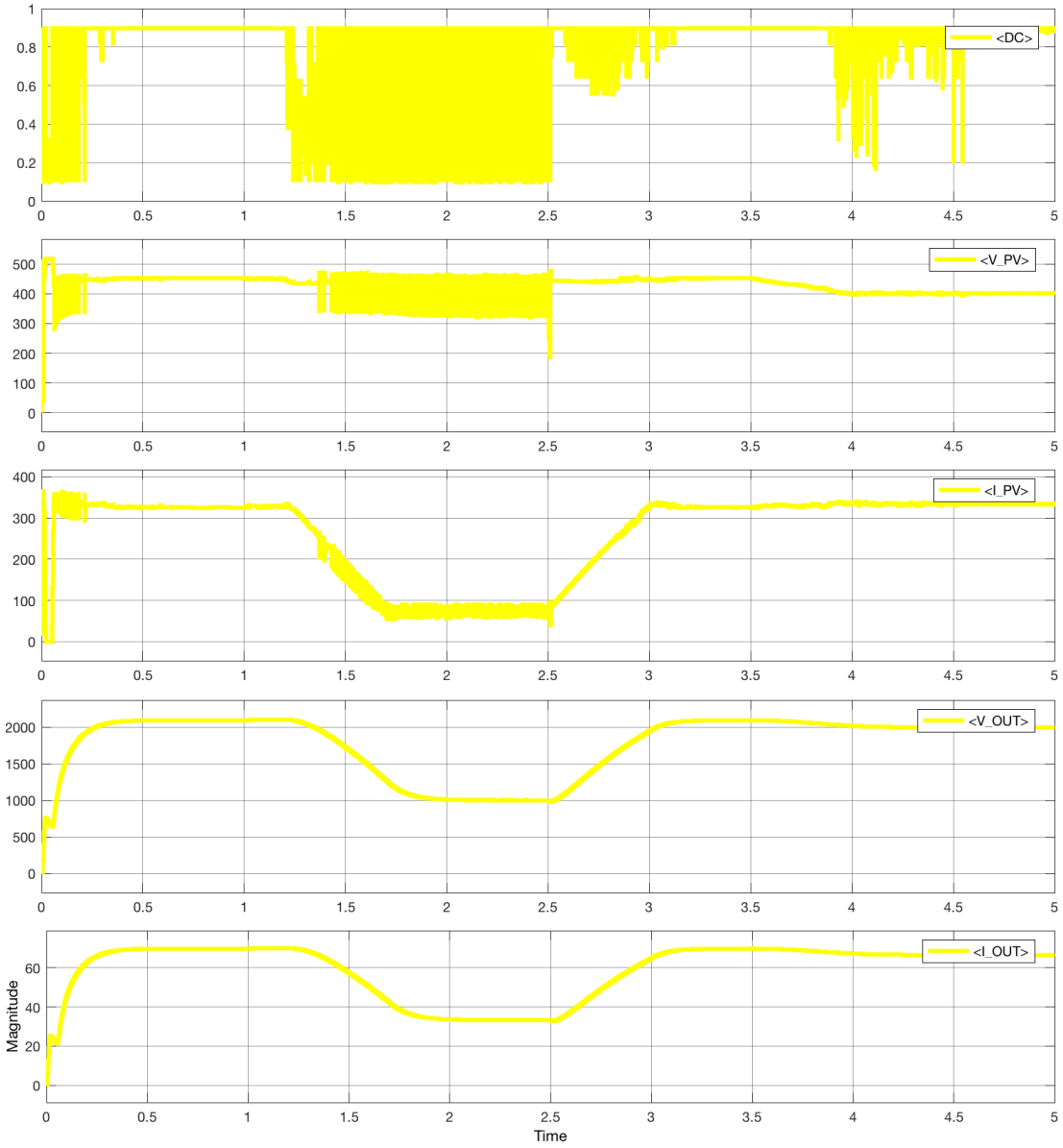

Figure 5.15 FLC DC, Voltage, and Current Diagrams Under Varying Conditions

Chapter 6 Conclusion

6.1 Research Objectives

This research focused on the Maximum Power Point Tracking ability of a PV system in order to determine the best possible method that can be used to generate the optimum levels of power. This is intended to help decision-makers and solar energy users understand how maximum power point tracking works, what factors affect it, and how to enhance its efficiency.

The objectives of this research were: (1) to analyze multiple controllers in terms of their Maximum Power Point Tracking ability when subjected to constant and varying weather conditions (partial shading); and (2) study the effect of irradiance and temperature change on the power output of a PV solar array. This was performed through modeling and simulating three controllers, which are P&O, INC + IR, and FLC, and comparing between them under two separate scenarios. The first scenario was simulated under constant conditions of irradiance and temperature while the second scenario was simulated under varying conditions of irradiance and temperature. Since P&O and INC are reported to have similar efficiency percentages as discussed in [39], this Thesis added an Integral Regulator to the INC in order to evaluate the difference in efficiency between the P&O and INC + IR. This thesis offers an analytical and methodological approach to realizing the qualitative differences between the common MPPT techniques and how the enhancement of the design will affect the output. It also aims at researching Artificial Intelligence techniques such as Fuzzy Logic as they are projected to be the core of our technology in the future. The following section reports on the findings of these two scenarios for each controller.

6.2 Summary of Research Results

6.2.1 Results of Constant Conditions – Scenario 1

This section discusses the results of the modeling and simulation for the three controllers under constant conditions of irradiance and temperature. Table 9.1 presents the rise time, settling time, and mean efficiency. The rise time is the time it takes the curve to get from 10% to 90% of its steady-state value while the settling time is the time is takes the curve to reach 90% of its steady-state value. It can be observed that the INC + IR has the longest rise time but still close to the other two controllers performances. Moreover, the INC + IR has the longest settling time with a bigger difference compared to the difference in rise time relative to the other controllers. This is due to the addition of the integral regulator, which is a known flaw of the IR where it reduces the steady-state error at the expense of the settling time. The mean efficiency is highest for the FLC, followed by the P&O and INC + IR, which have very similar values.

Table 6.1 Comparison Between the Controllers Under Constant Conditions

Controllers	Rise time (Seconds)	Settling time (Seconds)	Mean Efficiency %
P&O	0.197	0.26	96.40
INC + IR	0.216	0.8	96.06
FLC	0.198	0.26	98.66

6.2.2 Results of Varying Conditions – Scenario 2

This section describes the results of the modeling and simulation for the three controllers under varying conditions of irradiance and temperature. There are four periods in this case; each one corresponds to a change in either the irradiance or temperature. Period A represents a fixed value of irradiance and temperature at 1000

W per square meter and 25 ℃ respectively. In Period B the temperature remains unchanged, however, the irradiance drops from 1000 to 250 W per square meter and remains this way from the 1.7-second mark until 2.5 seconds. Period C commences after the 2.5 second mark, increasing the voltage back to 1000 W per square meter. Finally, in period D, the first change in the temperature is witnesses from 25 ℃ to 50 ℃ while having an irradiance of 1000 W per square meter (as shown in Table 8.1).

Table 6.2 presents the efficiency percentage in each of the four periods. In periods A, C, and D, the FLC controller shows superior efficiency percentages over the remaining controllers. However, in period B, INC + IR shows a superior efficiency percentage over the remaining controllers by an increase of 4.06% compared to the FLC and 33.68% compared to the P&O. The largest difference between percentages is noticed in Period B, which is due to the drop in solar irradiance from 1000 to 250 W per square meter. Finally, the mean efficiency percentage shows that the FLC has the highest percentage compared to the P&O and INC + IR.

Table 6.2 Comparison Between the Controllers Under Varying Conditions

Controllers	Period A Efficiency %	Period B Efficiency %	Period C Efficiency %	Period D Efficiency %	Mean Efficiency %
P&O	96.08	62.81	95.88	97.27	88.01
INC + IR	95.61	96.49	95.68	95.71	95.87
FLC	98.00	92.43	97.74	98.97	96.79

6.2.3 Comparison between Controllers' Characteristics

This section compares between the three controllers with respect to the mathematical model dependancy, number of oscillations, and implementation complexity as shown in Table 6.3.

Table 6.3 Comparison Between Controllers' Characteristics

Controllers	Mathematical Model	Number of Oscillations/second	Implementation Complexity
P&O	Required	550	Lowest
INC + IR	Required	90	Medium
FLC	Not Required	137	Highest

The first comparison between the three controllers' characteristics is the dependency of the controller on Mathematical models. Both, P&O and INC+IR require the existence of a mathematical model to program and fine-tune the controllers. However, FLC has the ability to perform without it, which makes fuzzy logic a very powerful and robust controller whenever there are inaccurate variables in the design. The second characteristic is the number of oscillations. This was high for the P&O and low for the two remaining controllers. Normally, a hill-climbing method would have high oscillations, however, the addition of the integral regulator has minimized the oscillations for the INC controller. Hence, as shown in Table 6.3, INC+ IR had the lowest number of oscillations per second, which is 90, followed by FLC with 137, and finally as expected P&O with a massive 550 oscillations per second. The last characteristic is the implementation complexity, which refers to how complex the installation is and how much it costs. P&O has the lowest installation complexity, as it only requires the use of one sensor. INC is usually considered to have a low

complexity but the addition of the integral regulator increases the system's complexity. FLC has the highest implementation complexity. In terms of cost, it is difficult to get an accurate monetary value with the ever-decreasing prices of the electronics; however, FLC generally has the highest cost [40].

6.3 Recommendations for Future Work

Recommendations for future work include expanding the testing range of the atmospheric temperature below 25 ℃ and above 50 ℃ as some parts of the world reach these temperatures such as some countries in Europe and in the Middle East respectively. Another point is to study the effect of changing both the temperature and irradiance at the same time as that may occur in some instances and study its effect on the output power. Moreover, another recommendation is to enhance and compare the results of both the P&O algorithm and FLC by adding an integral regulator to P&O and adding PID controller to FLC and making it an adaptive FLC. Another, recommendation is to increase the number of rules used in FLC and study the effect on output efficiency. A final further work recommendation is to connect the PV standalone system to the grid and make the necessary adjustments to the system, so that a more comprehensive result of the actual generated electricity can be reached.

References:

[1] U.S Department of Energy, Smart Grid: an introduction. [Online]. Available: https://energy.gov/oe/downloads/smart-grid-introduction

[2] "What is the Smart Grid?" SmartGrid.gov. [Online]. Available: https://www.smartgrid.gov/the_smart_grid/smart_grid.html. [Accessed: 20-Feb-2018].

[3] Nema, "Smart Grid: What is it and why is it important?," NEMA - Setting Standards for Excellence. [Online]. Available: https://www.nema.org/Policy/Energy/Smartgrid/Pages/default.aspx. [Accessed: 20-Feb-2018].

[4] DEWA, Powering Dubai on a smart, renewable grid, Smartdubai.ae, May 2014. [Online]. Available: http://www.smartdubai.ae/partner_story_two.php. [Accessed: 23-Feb- 2018].

[5] WiMax Forum, System Profile Requirements for Smart Grid Applications, February 05,2013. Available: http://files.wimaxforum.org/Document/Download/WMF-T31-002R010v01 Wimax_System_Profile_Requirements_for_SmartGrid_Applications

[6] "Power Systems Simulation Laboratory," A comparison between conventional grid and the Smart Grid | Power Systems Simulation Laboratory. [Online]. Available: http://www.itee.uq.edu.au/pssl/drupal7_with_innTheme/?q=node%2F347. [Accessed: 20-Feb-2018].

[7] C. P. Vineetha and C. A. Babu, "Smart grid challenges, issues and solutions," 2014 International Conference on Intelligent Green Building and Smart Grid (IGBSG), 2014.

[8] "Photovoltaic Solar Electric", SEIA. [Online]. Available: https://www.seia.org/initiatives/photovoltaic-solar-electric. [Accessed: 12- Mar- 2018].

[9] "Solar Photovoltaic System Design Basics", Energy.gov, 2013. [Online]. Available: https://energy.gov/eere/solar/articles/solar-photovoltaic-system-design-basics. [Accessed: 12- Mar- 2018].

[10] Energy Informative, 2013.

[11] Solarvis Energy , "Advantages and disadvantages of Solar Photovoltaic | Solar Energy News", Solarvis.energy. [Online]. Available: https://www.solarvis.energy/advantages-and-disadvantages-of-solar-photovoltaic/. [Accessed: 12- Mar- 2018].

[12] S. Sundaram, K. Sheeba and J. Babu, "Grid Connected Photovoltaic Systems: Challenges and Control Solutions - A Potential Review", International Journal of Electronics and Electrical Engineering, pp. 463-473, 2016.

[13] E. Camacho, T. Samad, M. Sanz and I. Hiskens, Control for Renewable Energy and Smart Grids. IEEE.

[14] J. Wippler, "» MPPT hunting » JeeLabs", Jeelabs.org, 2013. [Online]. Available: https://jeelabs.org/2013/05/21/mppt-hunting/. [Accessed: 09- Jan- 2019

[15] D. Bromberg, "Install tip: Know how inverter MPPT functionality affects performance", Solar Power World, 2018. [Online]. Available: https://www.solarpowerworldonline.com/2018/03/install-tip-inverter-mppt-functionality-affects-performance/. [Accessed: 09- Jan- 2019]

[16] Nader Anani, M. Shahid, Omar Al-kharji, Joao Ponciano, "A CAD Package for Modeling and Simulation of PV Arrays under Partial Shading Conditions," Energy Procedia, Volume 42, 2013, Pages 397-405, ISSN 1876-6102,

https://doi.org/10.1016/j.egypro.2013.11.040. Available at: http://www.sciencedirect.com/science/article/pii/S1876610213017426

[17] G. Patel, D. Patel and K. Paghdal, "ANALYSIS OF P&O MPPT ALGORITHM FOR PV SYSTEM", International Journal of Electrical and Electronics Engineering (IJEEE), vol. 5, no. 6, pp. 1-10, 2016. Available: http://oaji.net/articles/2016/1879-1481110428.pdf. [Accessed 14 January 2019].

[18] A. Atallah, A. Abdelaziz and R. Jumaah, "IMPLEMENTATION OF PERTURB AND OBSERVE MPPT OF PV SYSTEM WITH DIRECT CONTROL METHOD USING BUCK AND BUCKBOOST CONVERTERS", Emerging Trends in Electrical, Electronics & Instrumentation Engineering, vol. 1, no. 1, 2014. Available: https://airccse.com/eeiej/papers/1114eeiej03.pdf. [Accessed 14 January 2019].

[19] C. Panchano, "PERTURB AND OBSERVE ALGORITHMS FOR DC LOAD SYSTEMS", Master's, Newcastle University, 2014.

[20] U. Patel, D. Sahu and D. Tirkey, "Maximum Power Point Tracking Using Perturb & Observe Algorithm and Compare With another Algorithm", International Journal of Digital Application & Contemporary research, vol. 2, no. 2, 2013. Available: http://ijdacr.com/uploads/papers/DhaneshwariSahu_paper.pdf. [Accessed 14 January 2019].

[21] R. Mayfield, "The Highs and Lows of Photovoltaic System Calculations", Electrical Construction & Maintenance (EC&M) Magazine, 2012. [Online]. Available: https://www.ecmweb.com/green-building/highs-and-lows-photovoltaic-system-calculations. [Accessed: 14- Jan- 2019].

[22] M. Chaaban, "Temperature and PV Performance Optimization | AE 868: Commercial Solar Electric Systems", E-education.psu.edu. [Online]. Available: https://www.e-education.psu.edu/ae868/node/878. [Accessed: 14- Jan- 2019].

[23] M. R. H. Bipu, S. M. S. M. Chowdhury, M. Dautta, M. Z. Nain and S. I. Khan, "Modeling and analysis of maximum power point tracking algorithms using MATLAB/Simulink," 2015 International Conference on Electrical Engineering and Information Communication Technology (ICEEICT), Dhaka, 2015, pp. 1-6. doi: 10.1109/ICEEICT.2015.7307412

[24] M. Abulkadir, A. Samosir, A. Yatim and S. Yusuf, A NEW APPROACH OF MODELLING, SIMULATION OF MPPT FOR PHOTOVOLTAIC SYSTEM IN SIMULINK MODEL, 8th ed. ARPN Journal of Engineering and Applied Sciences, 2013, p. 491.

[25] G. Siegfried, "Many-Valued Logic", The Stanford Encyclopedia of Philosophy (Winter 2017 Edition), Edward N. Zalta (ed.), Available: https://plato.stanford.edu/archives/win2017/entries/logic-manyvalued/.

[26] D. Dubois, F. Esteva, L. Godo and H. Prade, FUZZY-SET BASED LOGICS — AN HISTORY-ORIENTED PRESENTATION OF THEIR MAIN DEVELOPMENTS, 8th ed. Elsevier BV, 2007.

[27] B. Ankayarkanni and L. Ezel, "GABC based neuro-fuzzy classifier with multi kernel segmentation for satellite image classification", Biomedical Research, vol. 29, no. 21, 2016. Available: http://www.alliedacademies.org/articles/gabc-based-neurofuzzy-classifier-with-multi-kernel-segmentation-for-satellite-image-classification.html. [Accessed 14 January 2019].

[28] K. Thórisson and H. Vilhjálmsson, "Intro to AI: Fuzzy Logic", Ru.is, 2007. [Online]. Available: http://www.ru.is/faculty/thorisson/courses/v2007/gervigreind/FuzzyLogic.html. [Accessed: 14- Jan- 2019].

[29] B. Singh and A. Mishra, "Fuzzy Logic Control System and its Applications", IRJET, vol. 2, no. 8, 2015. [Accessed 14 January 2019].

[30] J. Paulusová, "Fuzzy logic autotuning methods for predictive controller", Posterus.sk, 2010. [Online]. Available: http://www.posterus.sk/?p=7961. [Accessed: 14- Jan- 2019].
[31] R. Vicerra et al., "A multiple level MIMO fuzzy logic based intelligence for multiple agent cooperative robot system", TENCON 2015 - 2015 IEEE Region 10 Conference, 2015. Available: 10.1109/tencon.2015.7372985 [Accessed 14 January 2019].
[32] C. Lee, Fuzzy Logic in Control Systems: Fuzzy Logic Controller-Part I, 20th ed. IEEE, 1990, pp. 404 -415.
[33] N. Hussein Selman, "Comparison Between Perturb & Observe, Incremental Conductance and Fuzzy Logic MPPT Techniques at Different Weather Conditions", International Journal of Innovative Research in Science, Engineering and Technology, vol. 5, no. 7, pp. 12556-12569, 2016. Available: 10.15680/ijirset.2016.0507069 [Accessed 10 January 2019].
[34] N. de Reus, Assessment of benefits and drawbacks of' using fuzzy logic especially in fire control systems, 35th ed. TNO, 1994.
[35] M. Quamruzzaman, , Nur, Matin, Mahmud, Alam, “Highly efficient maximum power point tracking using DC–DC coupled inductor single-ended primary inductance converter for photovoltaic power systems.” International Journal of Sustainable Energy. Vol.35. pp.1-19, 2014. DOI: 10.1080/14786451.2014.961922.
[36] "Detailed Model of a 100-kW Grid-Connected PV Array- MATLAB & Simulink", Mathworks.com, [Online]. Available: https://www.mathworks.com/help/physmod/sps/examples/detailed-model-of-a-100-kw-grid-connected-pv-array.html. [Accessed: 21- Jan- 2019].
[37] A. Pradhan and B. Panda, "A Simplified Design and Modeling of Boost Converter for Photovoltaic Sytem", International Journal of Electrical and Computer Engineering (IJECE), vol. 8, no. 1, p. 141, 2018. Available: 10.11591/ijece.v8i1.pp141-149 [Accessed 21 January 2019].
[38] R. Erickson and D. Maksimović, Fundamentals of power electronics, 2nd ed. New York: Kluwer Academic, 2004.
[39] D. Sera, L. Mathe, T. Kerekes, S. Spataru and R. Teodorescu, "On the Perturb-and-Observe and Incremental Conductance MPPT Methods for PV Systems", IEEE Journal of Photovoltaics, vol. 3, no. 3, pp. 1070-1078, 2013. Available: 10.1109/jphotov.2013.2261118 [Accessed 21 January 2019].
[40] A. Reza Reisi, M. Hassan Moradi and S. Jamasb, "Classification and comparison of maximum power point tracking techniques for photovoltaic system: A review", Renewable and Sustainable Energy Reviews, vol. 19, pp. 433-443, 2013. Available: 10.1016/j.rser.2012.11.052.

Appendix A:

P&O MATLAB Code:

```
function [D,V,P] = Thesis(Param, Enabled, V, I)
% MPPT controller based on the Perturb & Observe algorithm.
% D output = Duty cycle of the boost converter (value between 0 and
1)
%
% Enabled input = 1 to enable the MPPT controller
% V input = PV array terminal voltage (V)
% I input = PV array current (A)
%
% Param input:
Dinit = Param(1); %Initial value for D output
Dmax = Param(2); %Maximum value for D
Dmin = Param(3); %Minimum value for D
deltaD = Param(4); %Increment value used to increase/decrease the
duty cycle D
% ( increasing D = decreasing Vref )
%
persistent Vold Pold Dold;
dataType = 'double';
if isempty(Vold)
 Vold=0;
 Pold=0;
 Dold=Dinit;
end
P= V*I;
dV= V - Vold;
dP= P - Pold;
if dP ~= 0 && Enabled ~=0
 if dP < 0
 if dV < 0
 D = Dold - deltaD;
 else
 D = Dold + deltaD;
 end
 else
 if dV < 0
 D = Dold + deltaD;
 else
 D = Dold - deltaD;
 end
 end
else D=Dold;
end
if D >= Dmax || D<= Dmin
 D=Dold;
end
Dold=D;
Vold=V;
Pold=P;
```